Thermal Modeling of Electronics Inside a Truck Cabin

Master's thesis in Mobility Engineering

ASHIK ROY

DEPARTMENT OF MECHANICS AND MARITIME SCIENCES

CHALMERS UNIVERSITY OF TECHNOLOGY
Gothenburg, Sweden 2024
www.chalmers.se

Master's Thesis in Mobility Engineering

Thermal Modeling of Electronics Inside a Truck Cabin

ASHIK ROY

CHALMERS
UNIVERSITY OF TECHNOLOGY

Department of Mechanics and Maritime Sciences
Division of Vehicle Engineering and Autonomous Systems
Chalmers University of Technology
Gothenburg, Sweden 2024

Thermal Modeling of Electronics Inside a Truck Cabin
ASHIK ROY

Supervisor: Zenitha Chronéer, Volvo GTT
Examiner: Simone Sebben, VEAS, Chalmers University of Technology

Master's Thesis 2024
Department of Mechanics and Maritime Sciences
Chalmers University of Technology
SE-412 96 Gothenburg
Sweden
Telephone +46 31 772 1000

Typeset in LaTeX
Gothenburg, Sweden 2024

Thermal Modeling of Electronics Inside a Truck Cabin
ASHIK ROY

Department of Mechanics and Maritime Sciences
Division of Vehicle Engineering and Autonomous Systems
Chalmers University of Technology

Abstract

Electronic Control Units(ECUs) are critical components in trucks, which are required to be operated within specific temperature ranges to minimize its failure rates. Some of the ECUs have integrated safety functions, and failure of these could result in the breakdown of the vehicle. These are often mounted underneath the Instrumentation Panel(IP), a confined space that also houses other heat sources, complicating their thermal management. Therefore, to understand the thermal behavior of ECUs under various conditions, Computational Fluid Dynamics(CFD) was used.

The CFD model was used to study the effects of factors such as ambient temperature, recirculation, and vehicle velocity on the ECU's thermal performance. A Proportional-Integral(PI) controller was modeled to regulate the air temperature through the HVAC(Heating, Ventilation, and Air Conditioning) ducts to maintain the cabin temperature at 22°C. To prevent oscillations while solving, the temperature of air through the HVAC was updated every 50 iterations.

Recirculation, which enhances the mixing of air inside the IP, was shown to decrease the temperature of the ECU. The extent of this temperature reduction was found to be influenced by the ambient temperature. Based on the understanding of the operation of the HVAC system, it was concluded that the cooling performance of the ECU is critical in cold ambient conditions. It was observed that at an ambient temperature of 0°C, increasing the recirculation fraction from 0 to 0.8 reduced the ECU's maximum temperature by approximately 7°C.

Based on the study's findings, several cooling strategies were proposed to improve the thermal management of ECUs. Utilizing the existing fan of the ECU to enhance the mixing of air within the IP was shown to reduce the ECU's temperature by around 5°C. While, incorporating an additional fan provided an even greater reduction, lowering the temperature by approximately 8°C.

Keywords: CFD, ECU, HVAC, airflow, electronics, cabin, heat transfer, thermal management

Acknowledgements

I extend my deepest appreciation to Zenitha Chronéer for her invaluable guidance as my thesis supervisor. I am grateful to Prof. Simone Sebben for her insightful feedback as the examiner. I would like to thank Jerome Rosenwald for his support during onboarding. Special acknowledgment to Anandh Ramesh Babu and Bruno Bartolec for their inputs that contributed to the completion of this thesis. Lastly, I am indebted to my family for their unwavering support throughout my academic journey.

Ashik Roy, Gothenburg, June 2024

List of Acronyms

Below is the list of acronyms that have been used throughout this thesis listed in alphabetical order:

1D	1-Dimensional
CFD	Computational Fluid Dynamics
ECU	Electronic Control Unit
HTC	Heat Transfer Coefficient
HVAC	Heating, Ventilation and Air-Conditioning
IP	Instrumentation Panel
PCB	Printed Circuit Board
PI	Proportional-Integral
PID	Proportional-Integral-Derivative
SoC	System-On-Chip

Nomenclature

ϕ	Transport variable
S_x	Source term
ρ	Density
t	Time
dX	Differential of X
$\mathbf{u}$	Velocity
$\mathbf{T}$	Stress tensor
p	Pressure
f_b	Body force
$\mathbf{D}$	Rate of deformation tensor
E	Energy
R	Specific gas constant
R_u	Universal gas constant
M	Molecular weight
$\overline{X}$	Average of X
$\mathbf{q}$	Heat flux
k	Thermal conductivity
T	Temperature
R_{th}	Thermal resistance
ΔX	Change in X
h	Convective heat transfer coefficient
Re	Reynolds number
L	Characteristic length
μ	Absolute viscosity
c_p	Specific heat
ν	Molecular diffusivity

α	Thermal diffusivity
Pr	Prandtl number
Gr	Grashof number
Ra	Rayleigh number
β	Coefficient of volume expansion
Nu	Nusselt number
σ	Stefan-Boltzmann constant
$f.REC$	Recirculation fraction
e	Error
k_p	Proportionality gain
k_i	Integral gain
k_d	Derivative gain
ϵ	Emissivity
ω	Rotation speed
ψ	Volume flow rate
$\dot{m}$	Mass flow rate
$Q_{convective}$	Magnitude of heat transfer through cabin walls
$T_{ambient}$	Temperature of ambient
T_{max}	Maximum temperature of ECU
T_{HVAC}	Temperature of air that exits the HVAC system

Contents

List of Figures

List of Tables

1
Introduction

1.1 Background

Electronic Control Units (ECUs) are devices used to monitor and control signals, forming an integral part of modern automobiles. Failure of critical ECUs can lead to vehicle breakdowns, particularly those integrated with safety features. It has been reported that high temperature is a major reason for the failure of electronics[1]. As a result, the thermal management of the ECU is a matter of great concern in the automotive industry.

Firstly, to understand the thermal behavior of an ECU, a generic ECU based on a similar existing ECU is made. A preliminary study is done on the generic ECU model to understand the operating window of the ECU, based on variation in ambient temperature and fan speed.

Some ECUs are housed underneath the Instrumentation Panel (IP) of trucks. The confined space and presence of other heat sources make predicting the temperature distribution of ECUs challenging. Thus, the generic ECU model is integrated into a simplified truck cabin model beneath the IP. This approach allows for an examination of the temperature distribution of the ECU and the surrounding air under various cabin conditions.

Since the problem statement involves the fluid flow around solid components of complex geometries, and the exchange of energy between various regions in the domain, computational fluid dynamics(CFD) is the best method to tackle the problem. For this study, STAR-CCM+ 2402 is used for meshing and solving physics, and ANSA is used for geometry preparation. Using the mentioned tools, the study aims to develop a CFD model that accurately represents the thermal characteristics of the ECU and the surrounding air. This involves the development of a methodology for simulating electronic components, and truck cabins.

The study discusses various cooling strategies aimed at optimizing the thermal management of ECUs based on the analysis of simulations.

1.2 Limitations

- Only half of the truck cabin is used for cabin simulation. The effect of the heat generated by other heat sources is assumed to be local and hence ignored.
- Leakages from the cabin are neglected.
- Filters, recirculation flap, and blower of the HVAC system are not modeled.
- One-dimensional simplification of truck cabin walls.
- Radiative heat transfer to the ambient is considered to be negligible.
- Solar loads are not modeled.
- Only steady-state studies are conducted.

2

Theory

2.1 Governing Equations

The governing equations represent the mathematical formulation of fundamental laws of physics for fluid flow. The fluid element is considered as a continuum for the analysis, and the macroscopic properties of the fluid elements are considered unaffected by the presence of individual molecules.
A general transport equation for a general variable ϕ can be expressed in the following form[2],

$$\frac{\partial(\rho\phi)}{\partial t} + div(\rho\phi\mathbf{u}) = div(\Gamma grad\phi) + S_\phi \tag{2.1}$$

Computational fluid dynamics uses a finite volume approach to discretize the fluid domain. Therefore, the governing equations are integrated over control volumes(CV). The governing equations can be written for a control volume as follows,

$$\int_{CV} \frac{\partial(\rho\phi)}{\partial t} dV + \int_{CV} div(\rho\phi\mathbf{u}) dV = \int_{CV} div(\Gamma grad\phi) dV + \int_{CV} S_\phi dV \tag{2.2}$$

Using Gauss's divergence theorem, equation 2.2 can be rewritten in terms of the bounding surface of the control volume.

$$\int_{\Delta t} \left(\int_{CV} \frac{\partial(\rho\phi)}{\partial t} dV \right) dt + \int_{\Delta t} \int_A \mathbf{n}.(\rho\phi\mathbf{u}) dA dt = \int_{\Delta t} \int_{CV} \mathbf{n}.(\Gamma grad\phi) dA dt + \int_{CV} S_\phi dV \tag{2.3}$$

2.1.1 Continuity

The continuity equation is the formulation of the law of mass conservation. In reference to the general transport equation, ϕ and S_ϕ become 1 and 0 respectively. The general form of the continuity equation is,

$$\frac{\partial\rho}{\partial t} + div(\rho\mathbf{u}) = 0 \tag{2.4}$$

2.1.2 Momentum

Momentum equations represent Newton's second law of motion, which states that the net force acting on a body is equal to the rate of change of momentum of the body. In reference to the general transport equation, ϕ becomes $\mathbf{u}$. For a fluid

element, the forces acting on it can be divided into body forces and surface forces. The momentum equation can be written as,

$$\frac{\partial(\rho \mathbf{u})}{\partial t} + \nabla.(\rho \mathbf{u}\mathbf{u}) = -\nabla.(p\mathbf{I}) + \nabla.\mathbf{T} + \mathbf{f}_b \tag{2.5}$$

For Newtonian fluid, the stress can be expressed in terms of the rate of deformation tensor as follows[3],

$$\mathbf{T} = 2\mu\mathbf{D} - \frac{2}{3}\mu(\nabla.\mathbf{u})\mathbf{I} \tag{2.6}$$

$$\mathbf{D} = \frac{1}{2}(\nabla\mathbf{u} + (\nabla\mathbf{u})^T) \tag{2.7}$$

2.1.3 Energy

The energy equation represents the first law of thermodynamics. It is expressed as follows,

$$\frac{\partial(\rho E)}{\partial t} + \nabla.(\rho E\mathbf{u}) = \mathbf{f}_b.\mathbf{u} + \nabla.(\mathbf{u}.\sigma) - \nabla.\mathbf{q} + S_E \tag{2.8}$$

2.2 Ideal Gas Equation

Ideal gas equation represents the relation between the state variables(pressure, temperature, and density) of an ideal gas. The equation is as follows,

$$\rho = \frac{p}{RT} \tag{2.9}$$

$$R = \frac{R_u}{M} \tag{2.10}$$

R_u – Universal gas constant$(= 8314.462 J/kmol.K)$

2.3 RANS Turbulence Models

Turbulent flows are fluid flows characterized by random and chaotic variations in velocity and all other flow properties. Rather than resolving all the length and time scales of a turbulent flow, turbulence models represents the flow in terms of time-averaged values.

$$\phi = \bar{\phi} + \phi' \tag{2.11}$$

On averaging, the Navier-Stokes equations can be represented as follows,

$$\frac{\partial(\rho \bar{\mathbf{u}})}{\partial t} + \nabla.(\rho \bar{\mathbf{u}}\bar{\mathbf{u}}) = -\nabla.(\bar{p}\mathbf{I}) + \nabla.(\bar{\mathbf{T}} + \mathbf{T_{RANS}}) + \mathbf{f}_b \tag{2.12}$$

The additional stress term in the Reynolds-Averaged Navier-Stokes equation is the turbulent stresses, and various closure models are used to model the turbulent stresses. Eddy viscosity models are based on the analogy between viscous stresses

and Reynolds stresses on the mean flow. The Boussinesq hypothesis states that the Reynolds stresses are proportional to mean rates of deformation[2].

$$\mathbf{T_{RANS}} = 2\mu_t \mathbf{D} - \frac{2}{3}(\mu_t \nabla . \bar{\mathbf{u}})\mathbf{I} \tag{2.13}$$

k-ϵ model is a commonly used turbulence model where the turbulent viscosity is expressed in terms of the turbulent kinetic energy and turbulent dissipation rate. The transport equations of these two parameters need to be solved in addition to the previously mentioned equations to capture the fluid flow.

2.4 Modes of Heat Transfer

Heat is a form of energy transfer that occurs due to the difference in temperature between two bodies. Transfer of thermal energy can take place via three different modes.

2.4.1 Conduction

Conduction is the transfer of thermal energy from more energetic particles to less energetic particles through interaction between the particles. The transfer of energy is diffusive through random molecular motion, and particles have no bulk motion. Fourier's law of conduction is the constitutive relation for conduction through a body. It is expressed as follows,

$$\mathbf{q} = -k\nabla T \tag{2.14}$$

Heat transfer through bodies that can be considered as 1-dimensional(1D) can be expressed in terms of thermal resistance. Thermal resistance is expressed as,

$$R_{th} = \frac{x}{k} \tag{2.15}$$

x – Thickness of body

For composite parts in series where heat conduction can be assumed to be 1D, an equivalent thermal resistance can be computed using the following relation,

$$R_{eq} = \sum_{i}^{n} R_i \tag{2.16}$$

R_i – Thermal resistances of individual parts

The heat flux through the 1D body can be expressed using the following equation,

$$q = \frac{\Delta T}{R_{th}} \tag{2.17}$$

ΔT – Temperature difference across the thickness of the body

2.4.2 Convection

Convection is the transport of thermal energy due to the bulk motion of the fluid. It involves the combined effect of conduction and fluid motion. Newton's law of cooling is used to express the convective heat flux transferred by a body to the surrounding fluid.

$$q = h(T_s - T_\infty) \tag{2.18}$$

h – Convective heat transfer coefficient
T_s – Temperature of solid surface
T_∞ – Bulk fluid temperature

2.4.2.1 Reynolds Number

Reynolds number is a non-dimensional number that determines the flow regime of the fluid flow. It is the ratio of inertial force to viscous force in a fluid.

$$Re_L = \frac{\rho V L}{\mu} \tag{2.19}$$

V – Fluid velocity

2.4.2.2 Prandtl Number

Prandtl number is a non-dimensional parameter that represents the relative thickness between the velocity and thermal boundary layer. It is defined as the ratio of molecular to thermal diffusivities.

$$Pr = \frac{c_p \mu}{k} = \frac{\nu}{\alpha} \tag{2.20}$$

2.4.2.3 Grashof Number

Grashof number is a non-dimensional parameter that is defined as the ratio of the buoyancy force to the viscous force acting on the fluid. It is used in cases where the heat transfer is predominantly due to natural convection.

$$Gr_L = \frac{g\beta(T_s - T_\infty)L_c^3}{\nu^2} \tag{2.21}$$

2.4.2.4 Nusselt Number

Nusselt number is a non-dimensional number that measures the convective heat transfer occurring at the surface of a body. It is defined as the ratio of convection to pure conduction heat transfer across the same fluid layer.

$$Nu_L = \frac{hL}{k_f} \tag{2.22}$$

k_f – Thermal conductivity of fluid

Average convective heat transfer coefficient of a surface can be obtained from the average Nusselt number, which can be expressed as a function of Re_L and Pr.

$$Nu = \frac{hL}{k_f} = f(Re_L, Pr) \tag{2.23}$$

2.4.2.5 Rayleigh Number

The Rayleigh number is a dimensionless parameter defined as the product of Gr and Pr. It is commonly used in empirical correlations of Nu in the case of natural convection.

$$Ra_L = Gr.Pr \tag{2.24}$$

$$Nu = CRa_L^n \tag{2.25}$$

2.4.3 Radiation

Radiation is a mode of heat transfer where thermal energy is transferred through electromagnetic radiation between bodies at different temperatures. Unlike the other modes of heat transfer, radiation does not require a medium to transport thermal energy.

2.4.3.1 Blackbody Radiation

A black body is a perfect emitter and absorber of radiation. The radiation emitted by a black can be expressed in terms of Stefan-Boltzmann's law as,

$$q = \sigma T^4 \tag{2.26}$$

σ – Stefan-Boltzmann constant ($= 5.670 \times 10^{-8}\ W/m^2.K^4$)

2.4.3.2 Surface-to-Surface Radiation

Radiation transferred between bodies due to their temperature falls between 0.1 to 100 μm, and is known as thermal radiation.
Electromagnetic radiations of this frequency do not transmit through opaque objects, but partially through translucent and transparent bodies. Hence, radiation is a volumetric phenomenon for transparent and translucent bodies, while it is considered a surface phenomenon for opaque objects.
Gray bodies exhibit radiative properties that remain the same across all wavelengths. In contrast, diffuse bodies emit radiation uniformly in all directions.
Emissivity represents the ratio of radiation emitted by a surface at a given temperature to the radiation emitted by a black body at the same temperature.

Emissive power of a grey body with emissivity ϵ can be expressed as,

$$q_{grey} = \epsilon(\sigma T^4) \tag{2.27}$$

Absorptivity is the fraction of incident radiation that is absorbed by the surface.

$$\alpha = \frac{Absorbed\,radiation}{Incident\,radiation} \tag{2.28}$$

Reflectivity is the fraction of incident radiation that is reflected by the surface.

$$\rho = \frac{Reflected\,radiation}{Incident\,radiation} \tag{2.29}$$

Transmissivity is the fraction of incident radiation that is transmitted through the surface.

$$\tau = \frac{Transmitted\,radiation}{Incident\,radiation} \tag{2.30}$$

Radiative heat transfer between surfaces is influenced by their relative orientations. To accommodate this, a parameter known as the view factor is introduced. It is defined as the fraction of radiation leaving a surface that strikes another surface directly. It is expressed as follows,

$$F_{12} = \frac{1}{A_1}\int_{A_2}\int_{A_1}\frac{cos\theta_1 cos\theta_2}{\pi r^2}dA_1 dA_2 \tag{2.31}$$

2.5 HVAC System

The HVAC(Heating, Ventilation, and Air Conditioning) system of a vehicle is used to maintain the temperature, humidity, and air distribution within the cabin to meet the passengers' comfort requirements under different ambient conditions. For this study, the HVAC system on the cabin side is only of interest, Fig. 2.1. The key components that comprise the system are,

- Heater - It is used to heat the air to required temperatures, either electrically or by using waste heat.
- Evaporator - It is used to cool the air and also to dehumidify fresh and recirculated air.
- Blower - It is used to control the mass flow flowing through the HVAC ducts.
- Filters - Filters are used to filter out air pollutants in the air, both fresh and recirculated.
- Ducts - To attain different air distribution depending on ambient conditions and passenger requirements, there are multiple vents on the vehicle that are connected to the HVAC system through ducts.
- Flaps - It is used to control the temperature of the HVAC air by mixing and in the air distribution in different ducts.

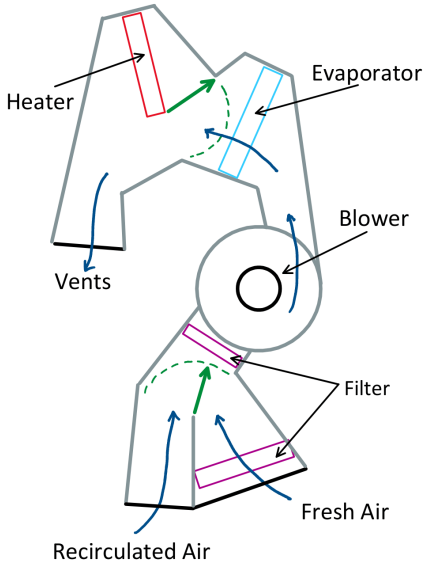

Figure 2.1: Schematic of HVAC system

Recirculation is a technique used to reduce the energy consumption of the HVAC system by taking a portion of the cabin air back to the HVAC system without taking in fresh air from the ambient, Fig. 2.2.

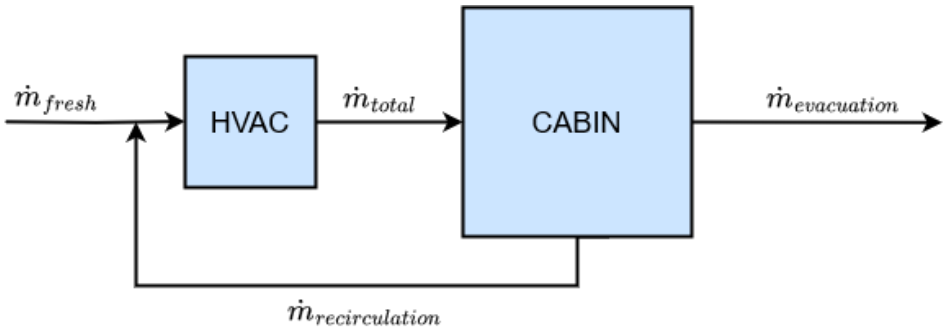

Figure 2.2: Schematic of recirculation

The ratio of the mass flow of air that is recirculated to the total mass flow flowing through the HVAC system is called the recirculation fraction[4].

$$f.REC = \frac{\dot{m}_{recirculation}}{\dot{m}_{total}} \tag{2.32}$$

For cases where the ambient temperature is high, the recirculation fraction is close to 1. It is never set to unity as it would result in high CO_2 levels inside the cabin. In this scenario, most of the mass flow is directed through the face vents, as the cold air tends to descend due to buoyancy.
At cold ambient conditions, the humidity ratio is low[5], and the evaporator is turned off. Therefore, the recirculation can result in fogging of windows and windshield which will affect the driver's visibility. As a result, in cold ambient conditions, only

fresh air is taken in and the recirculation fraction is set to 0. Therefore, in such cold conditions, only fresh air is drawn in, and the recirculation fraction is set to 0. The majority of the airflow is then directed toward the floor, defroster, and demisters. Due to buoyancy, the rising hot air naturally mixes with the cabin air, aiding in the maintenance of an even overall cabin temperature.
The HVAC system has a controller that sets the total mass flow rate through ducts and the heat generated by the heater core to maintain the cabin temperature at a comfortable level, usually 22°C. It is a closed-loop controller that monitors the cabin temperature and adjusts the parameters based on simulation models.

2.6 Controller

Feedback can be defined as two or more strongly coupled dynamic systems in which each system influences the other systems.
A controller is a set of algorithms that sets the values of external inputs of a dynamic system to get a desired output, by sensing the output of the system and comparing it against desired values[6].

2.6.1 PID Controller

A PID controller is a feedback control system that continuously calculates and adjusts the control input to a process based on proportional, integral, and derivative terms, aiming to minimize the difference between the desired setpoint and the measured output.
The input-output relation of a PID controller can be expressed as follows,

$$u = k_p e + k_i \int e(t)dt + k_d \frac{de}{dt} \tag{2.33}$$

e – Error; the difference between the actual and the desired value
k_p – Proportionality gain
k_i – Integral gain
k_d – Derivative gain

Each term of the above equation serves the following purpose,

- Proportional term - Its function is to provide an immediate response to the current error.
- Integral term - It integrates the error signal over time, effectively accumulating error.
- Derivative term - It anticipates future trends in the error signal by responding to its rate of change.

3
Methods

3.1 ECU Modeling

A generic ECU model is developed to replicate an existing ECU's geometric dimensions. It is equipped with a centrifugal fan, and has fins on one side to efficiently dissipate heat generated by internal components into the surrounding environment as shown in Fig. 3.1. Subsequent investigations utilized this model to assess the temperature distribution within the ECU under various operational scenarios. It is assumed that all electronic components within the ECU must maintain a steady-state operating temperature below 120°C to ensure the longevity of the components.

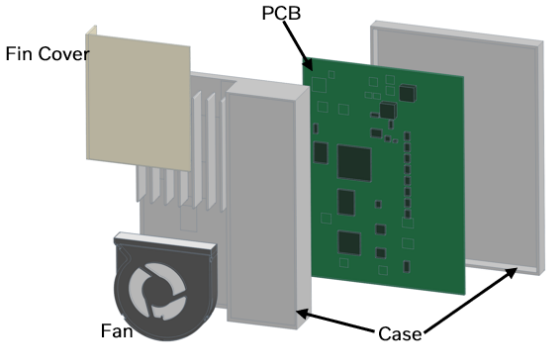

Figure 3.1: Exploded view of the generic ECU model used for the study

In this section, the various modeling parameters that are chosen to model the continua as accurately as possible are discussed. The continua can be broadly classified into two; solid and fluid.

3.1.1 Geometry

The key components of an ECU from a thermal modeling perspective are:

- Case
- Fan
- Printed Circuit Board(PCB)
- System-on-chip(SoC) and other heat-generating components
- Fan

The material properties for each solid component are detailed in Table 3.1. Since the PCB is a composite having materials of different thermal conductivities, an effective

thermal conductivity is defined. Within the PCB's plane, the thermal conductivity is higher (20 W/K.m), while across the PCB, it is lower (0.4 $W/K.m$)[3].

Component	Material	$k(W/K.m)$	ϵ
Case	Cast Aluminium	130	0.1
Fin Cover	Plastic	0.05	0.8
Electronic component	Aluminium Oxide	25	0.8
PCB	FR4-Cu	Orthotropic	0.8

Table 3.1: Material properties of various ECU components

The fan curve (Fig. 3.2) of a centrifugal fan is used for modeling the fan, and the fan can be operated at different rotational speeds based on the equations (3.1) and (3.2). The air inside the case is isolated from the surroundings, and the flow is assumed to be laminar.

$$\Delta P_2 = \Delta P_1 \left(\frac{\omega_2}{\omega_1}\right)^2 \left(\frac{T_1}{T_2}\right) \tag{3.1}$$

$$\psi_2 = \psi_1 \left(\frac{\omega_2}{\omega_1}\right) \tag{3.2}$$

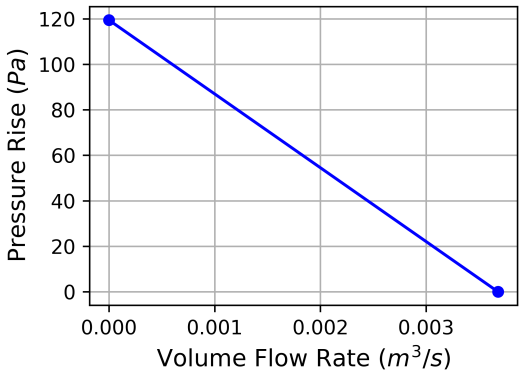

Figure 3.2: Fan curve at the rotation speed of 3400 rpm

All the components are assumed to be gray and diffuse, and the radiation is modeled using the surface-to-surface radiation model.

For all chips except the SoC, the heat generated by the components is modeled to be constant, ranging from 0.5 W to 2.5 W, as depicted in Fig. 3.3. The color coding and grouping are provided for illustrative purposes and do not precisely correspond to the heat generated by individual components.

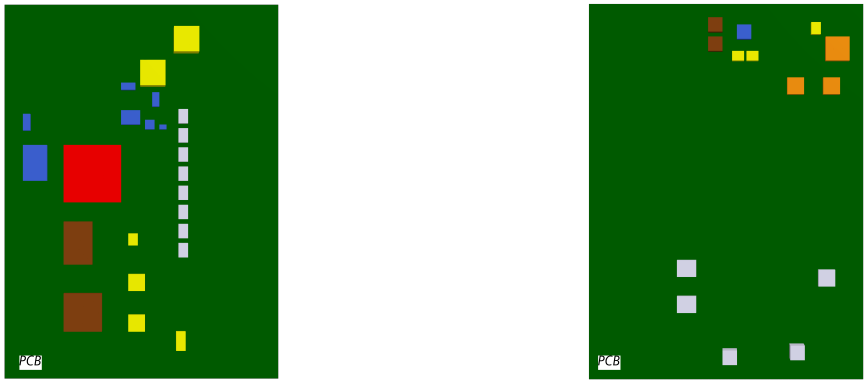

Figure 3.3: Components color-coded based on heat generation

Heat Loss (W)	Color
0.5	
1.0	
1.5	
2.0	
2.5	
Heat Function	

Table 3.2: Color code: Heat generated by ECU

For the SoC, heat generation is temperature-dependent, necessitating the creation of a function to model this variation, as illustrated in Fig. 3.4. Since all heat-generating components are modeled as solid blocks without resolving the junctions, the maximum temperature of the SoC is assumed to be the junction temperature for the study.

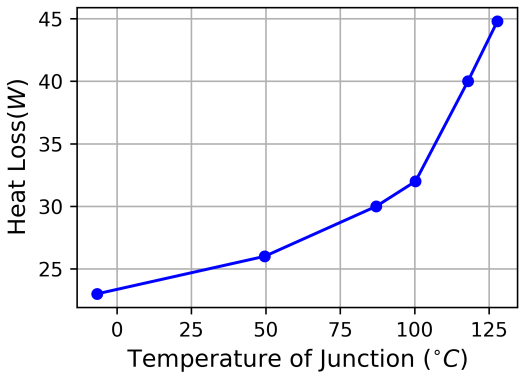

Figure 3.4: Variation of SoC heat loss with junction temperature

3.2 Preliminary Study

A parametric study is conducted using the generic ECU to understand the thermal behaviour of ECUs. For this, the ECU is kept in an enclosure of size $1.5m \times 1.5m \times 1.5m$ that has constant temperature boundaries. For the parametric study, the following operating conditions are checked.

- Fan Switched OFF - To check the operating window in case of natural convection
- Fan Switched ON - Standard operating case

The ECU is placed with an offset of 1m from the wall that faces the outlet of the fan as shown in Fig.3.5. This is to prevent any hot air that recirculates after hitting the wall from being sucked in by the fan, and it can be assumed that the temperature of the wall is the temperature of ambient air of the ECU.

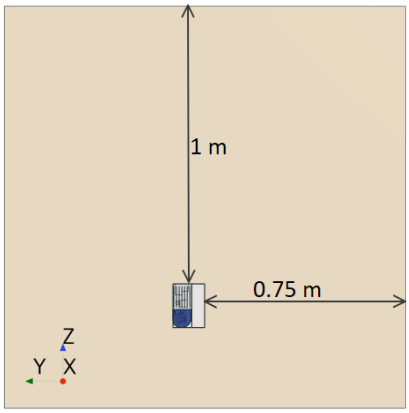

Figure 3.5: ECU in the enclosure

In the later stage of the study, the thermal characteristics of the ECU within the truck cabin will be analyzed. The Realizable k-ϵ turbulence model, which has demonstrated good correlation with measurements in truck cabin simulations [7], will be utilized. Consequently, the air surrounding the ECU is modeled using the Realizable k-ϵ turbulence model with Two-Layer All-y+ Wall Treatment. The density of air is modeled using the ideal gas equation, and gravity is applied in the negative z-direction. The reference pressure is set to 1 atm. Segregated solver is employed to solve both the flow and energy equations.

3.2.1 Mesh Study

Polyhedral cells are used to mesh both the fluid and solid regions. Thin mesh is used for the ECU Case, Fin Cover, and PCB. Prism layers are used for the turbulent air region to achieve a $y^+ \approx 1$. Since conformal mesh interfaces give the best solid-to-solid heat transfer[8], the ECU is meshed to be fully conformal. For the study, mesh generation of the domain is categorized into regions:

- Surface and Boundary Mesh
- Bulk Mesh

3.2.1.1 Surface and Boundary Mesh

The size of the surface mesh is chosen based on the part's dimensions and its significance in accurately predicting the engineering value of interest to the study, as well as ensuring the stability of the simulation. For this study, the temperature of the heat-generating parts is of interest, and the surface mesh of those components is refined.
Radiation patches are created from the faces of the geometry, and for the preliminary study, a patch-to-face proportion of 100 is chosen.
Prism layers are used to accurately capture the boundary layer flow, and therefore the thickness of the boundary needs to be computed. Boundary layer thickness for external flow can be computed using the expression,

$$\delta = \frac{0.37 L_c}{Re^{\frac{1}{5}}} \tag{3.3}$$

The gap(8.5 mm) between the two fins of the case is considered the characteristic length, and the velocity(6.5 m/s) of air when the fan is run at 4000 rpm is taken to calculate the Re. The boundary layer thickness is calculated to be 0.6 mm. Hence, a prism layer thickness of 1 mm is chosen as a safety margin. To achieve a $y^+ \approx 1$, 8 prism layers with a prism layer stretching of 1.2 is used[9], Fig. 3.6.

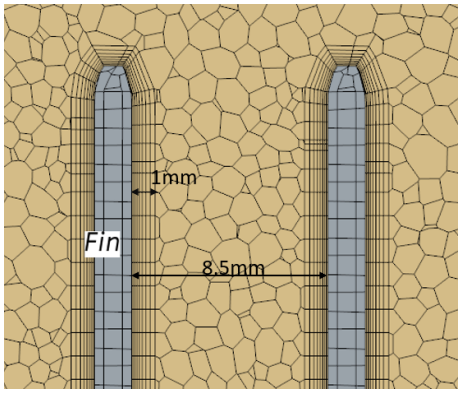

Figure 3.6: Prism layers of air in contact with ECU case

3.2.1.2 Bulk Mesh

The mesh consisting of cells located away from the boundary layer is referred to as the bulk mesh. Several factors, such as the specific region of interest within the mesh, the presence of notable gradients in field properties, and the overall dimensions of the computational domain determine the size of these cells. In areas where precise flow capture is crucial, volume metric refinement is applied to enhance accuracy.
Steady-state simulations are considered to be converged if the engineering quantities of interest have reached a steady-state value. In this study, convergence is verified by monitoring the maximum temperature of components and the volume-averaged temperature of the case. Additionally, a mesh sensitivity analysis is conducted to ensure the independence of results from bulk mesh size and to reduce the computational resource utilization for future simulations.

3.3 Cabin Modeling

For this investigation, only the ECUs located beneath the Instrumentation Panel(IP) are studied. This enclosed space has varying airflow rates and temperature due to the prescence of other components and is influenced by ambient conditions.. Understanding the temperature and fluid flow around the ECU is crucial for determining potential failure conditions. Therefore, a cabin study is essential to analyze the thermal behavior of the ECU and predict its operational limits.

3.3.1 Geometry

In this section, the various components that make up the cabin, and are necessary to be modeled to accurately represent the air around the ECU are discussed. To simplify the modeling process, only the right half of the cabin is considered for analysis. It is assumed that the impact of other heat sources within the cabin is localized and does not significantly influence airflow or temperature distribution around the ECU. The key components from a thermal modeling perspective that are modeled include,

- ECUs - Primary focus of analysis
- IP -Influences the temperature of the air around the ECU
- HVAC Ducts -Located near the ECUs
- Manikin - Impacts the overall cabin temperature
- Convective boundaries - Impacts the overall cabin temperature

Table 3.3 shows the material properties used for different solid parts.

Material	Component	k(W/K.m)	ϵ
Plastic	IP, Ducts	0.05	0.8
Glass	Windshield,Window	1.17	0.14
Composite	Cabin Walls	–	0.8

Table 3.3: Material properties of various cabin components

3.3.1.1 Instrumentation Panel

The ECUs are located underneath the IP, Fig. 3.7 and the heat generated by it results in the formation of a hot air pocket underneath the IP. Therefore, modeling of heat rejected through the IP to the cabin air is essential.

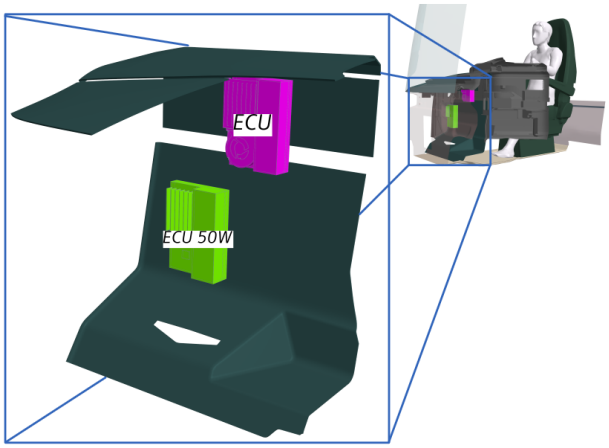

Figure 3.7: IP with ECUs beneath it

3.3.1.2 HVAC Ducts

The ECUs are close to the HVAC ducts, which affect the airflow and temperature around them, thus necessitating their inclusion in the model, Fig. 3.8. The recirculation of air within the cabin influences fluid flow around the ECU due to its proximity to the ECU as shown in Fig. 3.9, and is therefore accounted for in the modeling process. Since the focus is on the air surrounding the ECU, the flow distribution inside the HVAC system is less critical compared to the temperature of the duct itself. To simplify the model, the air filters in the recirculation ducts are disregarded, and the blower is represented by controlling the mass flow rate through the duct. The airflow rates through the other ducts are set based on typical climate cases for a full-cabin model, as shown in Table 3.5.

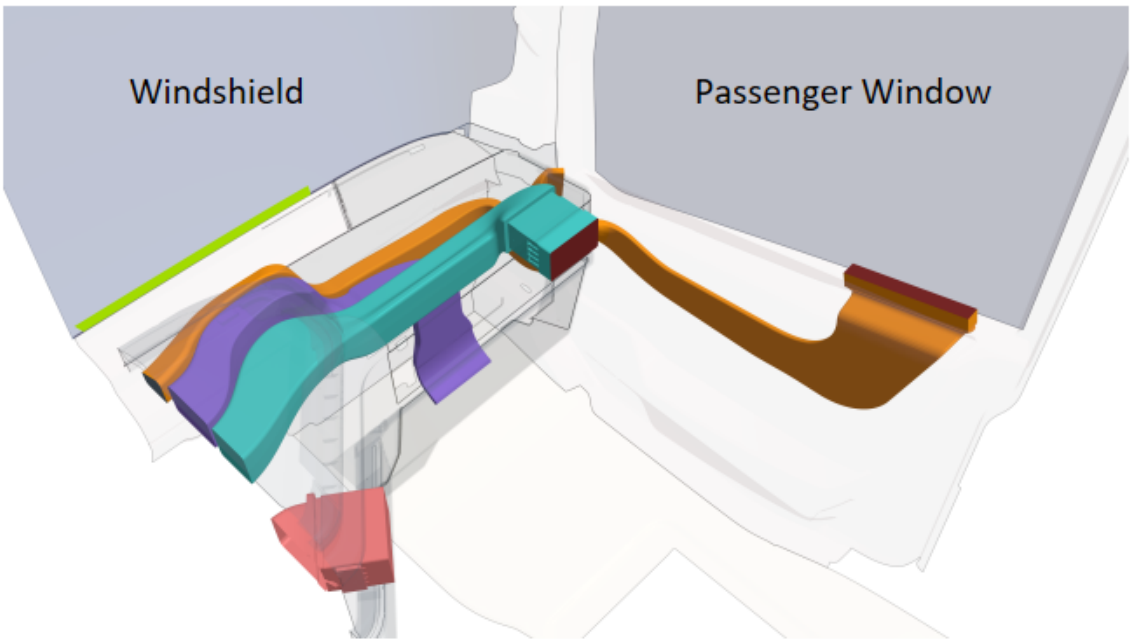

Figure 3.8: HVAC ducts that are modeled for the study

Component	Color
Duct left	
Duct right	
Duct floor	
Duct demist	
Vent defrost	

Table 3.4: Color code: HVAC ducts

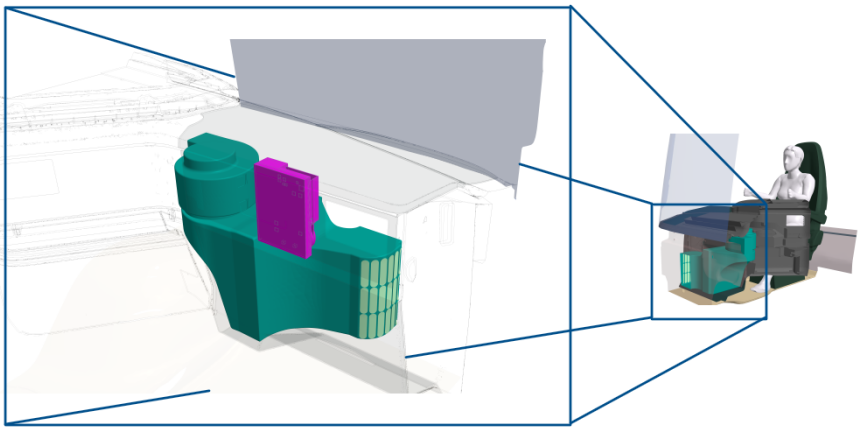

Figure 3.9: Recirculation duct and ECU

	Face Vent	Floor	Demist	Defrost	Total Mass Flow(g/s)
Cold Climate	3%	20%	9%	10%	83.1
Hot Climate	20%	3%	0%	0%	105.5

Table 3.5: Distribution of air through different ducts

The recirculation duct draws in a fraction of cabin air, determined by operating conditions, and the recirculation fraction is used to compute the mass flow of air through the recirculation ducts, and fresh air that is taken by the HVAC system. The following expression is used to compute the same,

$$\dot{m}_{recirculation} = f.REC \times m_{total} \tag{3.4}$$

$$\dot{m}_{fresh} = (1 - f.REC) \times m_{total} \tag{3.5}$$

As the thickness of the ducts (2 mm) is small, shell regions are employed for its modeling.

3.3.1.3 Cabin Walls

Heat in the cabin dissipates to the ambient environment either through the evacuation located behind the seats or is gained or dissipated via convection through the exterior cabin surfaces. Instead of individually modeling every solid component from the interior surface to the exterior cabin, a simplified 1D approach is adopted.

This involves calculating an equivalent thermal resistance for all the surfaces using equations 2.15 and 2.16. When there is an air gap between surfaces, equation 2.15 needs to be modified to account for the natural convection that occurs[10], using the following expression:

$$k_{eff} = Nu.k \tag{3.6}$$

In this study, the effective thermal conductivity is computed only for horizontal enclosures. The equation of Nu for horizontal enclosures, where the hot surface is on the bottom is used(3.7)[10]. If the hot surface is on the top, natural convection is insignificant, and Nu is taken as unity.

$$Nu = 1 + 1.44\left[1 - \frac{1708}{Ra_L}\right]^{+} + \left[\frac{Ra_L^{1/3}}{18} - 1\right]^{+} \tag{3.7}$$

Table 3.6 shows the thermal resistance values used for modeling the convective boundaries. Convection to the ambient is modeled by specifying an external heat transfer coefficient, which varies with vehicle speed, as shown in Fig. 3.10[7].

The difference between the wall temperature of the truck's exterior and the ambient temperature is assumed to be negligible for all surfaces. Therefore, heat transfer via radiation between the truck and the environment is neglected. To further simplify the model, solar loads are neglected for the study.

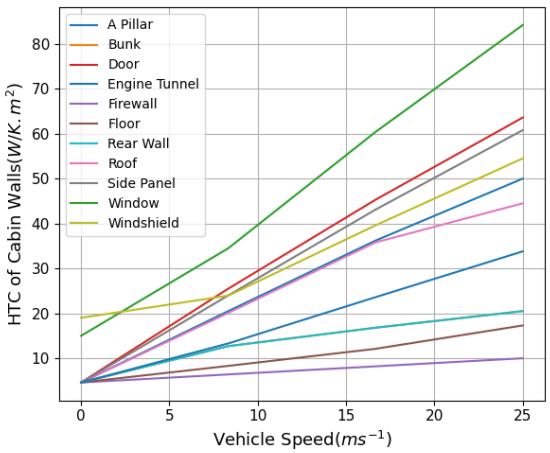

Figure 3.10: Variation of HTC of cabin walls with vehicle speed

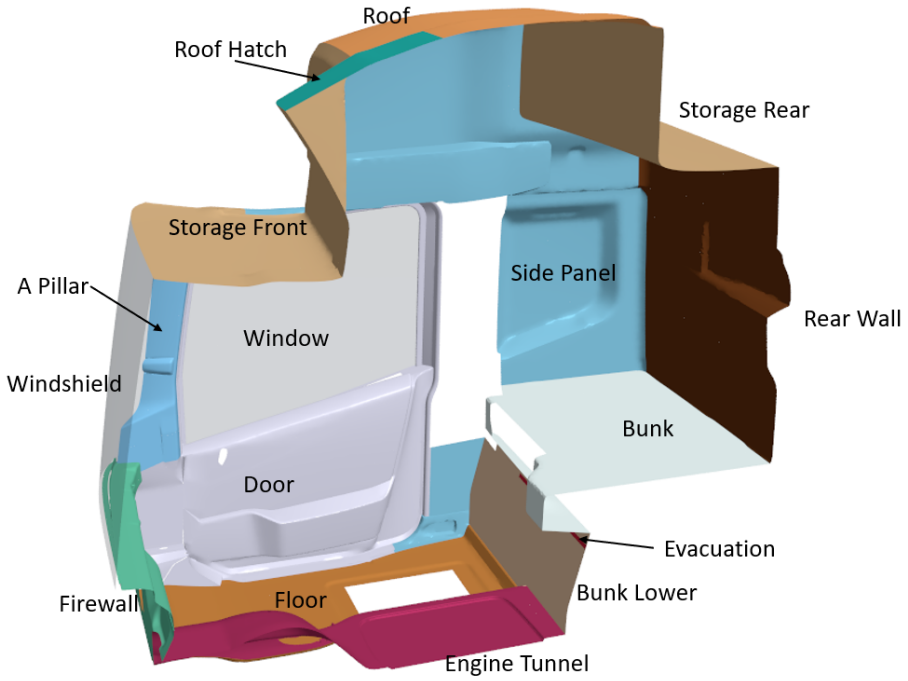

Figure 3.11: Cabin surfaces through which heat transfer occurs to ambient

Surface	Cold Climate($m^2.K/W$)	Hot Climate($m^2.K/W$)
Bunk Lower	31.7	31.7
Floor	1.19	1.19
Rear Wall	2.3	2.3
Door	5.5	5.5
Window	0.0042	0.0042
Engine Tunnel	1.33	1.33
Firewall	0.6	0.6
Windshield	0.0058	0.0058
Roof	1.2	1.2
Side Panel	3.16	3.16
Bunk	23.1	10.1
Roof Hatch	0.5	1.2
Front Storage	3.4	17.2
Rear Storage	3.4	17.2

Table 3.6: Thermal resistance of cabin walls

Additionally, the other surfaces of interest for modeling the cabin are discussed as follows. The manikin in the truck is modeled with a constant temperature of 30°C, and the evacuation pressure of the truck cabin is set to 1 atm. A constant heat source ECU that generates 50 W is placed next to the ECU of interest to better represent real-world conditions, as shown in Fig. 3.7.
The remaining surfaces in the truck, which are included to accurately model the flow inside the IP but do not influence the temperature of the air around the ECU, are

modeled as adiabatic walls, namely instrumentation panel support, curtain, harness, and seat. Lastly, the wall that splits the cab in half is modeled as a symmetry plane.

3.3.1.4 Fluid Region

The fluid flow inside the truck cabin is modeled using the k-ϵ turbulence model with Two-Layer All-y+ Wall Treatment, as it is considered robust for modeling indoor environments [11], and has shown good correlations with measurements for truck cabin simulations [7]. The truck cabin models are solved using a coupled solver.
The ideal gas equation is used to model the density of air, and gravity is considered in the negative z-direction. The reference pressure is set to 1 atm. All surfaces within the interior of the truck are assumed to be grey and diffuse. Internal radiation between surfaces in the truck cabin has been modeled using surface-to-surface radiation. A patch-to-face ratio of 25 is used to create the view factors for modeling radiation.

3.3.2 Mesh Study

For the cabin model, the meshing procedure outlined in section 3.2.1 is employed. Polyhedral mesh is used for the fluid regions in the cabin. Thin mesh cells are used to model the IP. Boundary layers are refined to achieve a y^+ ≈1. For the HVAC ducts, the width of the duct is taken as the characteristic length, and the velocity through the duct is taken as 5 m/s. A prism layer thickness of 3 mm with 8 layers is utilized for the ducts, while for most convective boundaries, 4 prism layers with a total thickness of 6 mm is employed[9].
The focus of the study is confined to the region underneath the IP.

3.3.3 Controller

The temperature of the cabin is kept close to 22°C at all ambient conditions to meet the comfort of the driver. Achieving this cabin temperature requires a coordinated adjustment of both the mass flow and the temperature of the air through the ducts. In this study, parameters such as ambient temperature, vehicle speed, and recirculation ratios are varied, all of which can impact the temperature of the air through the HVAC ducts. Consequently, an HVAC temperature controller is modeled to regulate the HVAC temperature and maintain the desired cabin temperature.
For simplification of the model, it is assumed that the mass flow through the ducts is fixed to specific values, one for the hot case and another for the cold case as shown in Table 3.5.
A PI controller with a gain of 0.3 for proportionality and 0.1 for the integral term is modeled[12]. The controller logic can be expressed as follows,

$$T_{update} = T_{intial} + k_p.e + k_i \sum e_i \tag{3.8}$$

T_{update} – Updated temperature of HVAC air
T_{initial} – Initial guessed temperature of HVAC air
e – Difference between the current temperature and the required temperature

The reference temperature, essential for computing the error, is determined as the volume average of air within a sphere of radius 200 mm positioned above the IP, as illustrated in Fig. 3.12. This temperature is assumed to represent the average cabin temperature for modeling the controller. The utilization of volume averaging helps to minimize oscillations in the controller. Additionally, to further prevent oscillations, the temperature of the HVAC air is updated every 50 iterations.

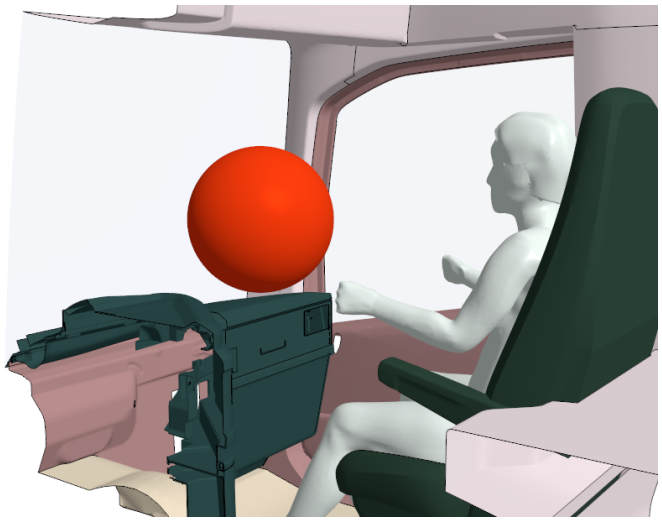

Figure 3.12: Sphere used to compute the cabin temperature for the controller

3.3.4 Validation of the CFD Model and Controller

Before simulating different cases with ECU inside the truck, the CFD model is validated with measurement data of a similar truck model. To match the model with the measurements, the manikin and the ECUs are removed from the model to replicate the measurement setup of the truck cabin. For the validation, two ambient temperature scenarios are considered: one for hot conditions, and one for cold conditions. In both cases, the controller is set to regulate the cabin temperature.

In the simulation, probes are placed at locations within the cabin that could influence the temperature of the ECU, specifically the region above the IP, the floor, and the passenger as shown in Fig. 3.13. The temperature of the air at the location of these probes is then compared against the measurements to validate the model. The uncertainity in the measurement is $\pm 0.5°C$.

To validate the controller, the cabin temperature is monitored to ensure it reaches a steady-state value and achieves the desired set value.

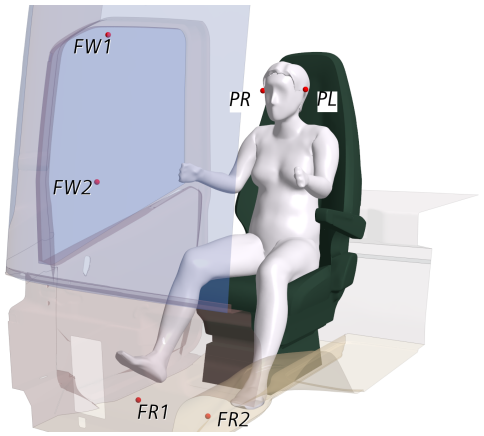

Figure 3.13: Probes used to validate the simulation

3.4 Cabin Study

After validating the cabin and controller models, the cabin model is used to conduct a parametric study investigating the thermal response of the ECU under various conditions. The key parameters analyzed include:

- Ambient Temperature
- Recirculation Fraction
- Vehicle Speed

The parametric study is divided into two main categories: hot climate and cold climate. The parameters mentioned above are examined within these two broad categories.
Based on the observations from the parametric study, several methods to improve the cooling performance of the ECU are discussed at the end of the section.

The section views used for post-processing the simulations are illustrated in Fig. 3.14. Each section plane is labeled based on the direction of its normal vector. The X-plane illustrates the region within the IP. The Y-plane, intersecting the ECU, offers context about the airflow and temperature of the region surrounding the ECU. The Z-plane shows the cross-sectional view of the recirculation duct.

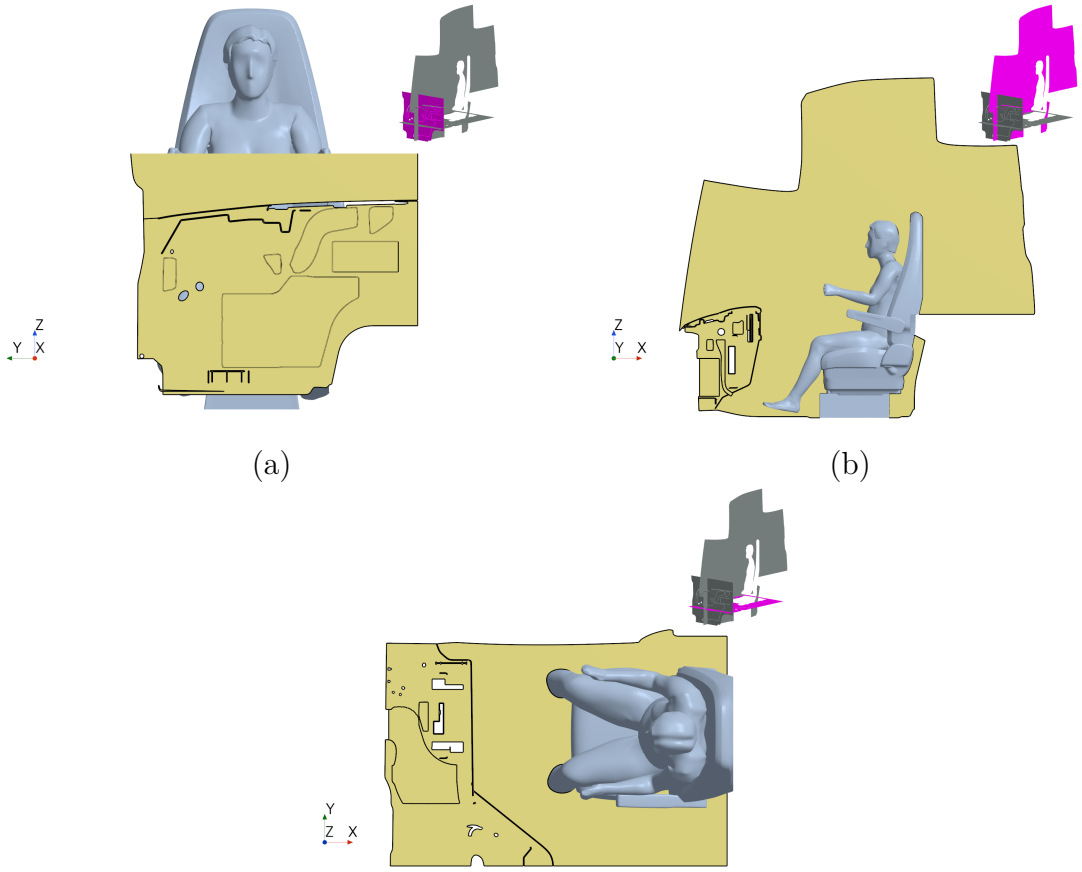

(a) (b)

(c)

Figure 3.14: Section planes used for post-processing. (a)X-plane. (b)Y-plane. (c)Z-plane.

4
Results

4.1 Preliminary Study

4.1.1 Mesh Study

For conducting the mesh sensitivity analysis, three different base sizes are simulated for both solid components and fluid domains. For the solid components and air within the ECU, base sizes of 1 mm, 3 mm, and 5 mm are considered. Meanwhile, for the air region surrounding the ECU, base sizes of 10 mm, 20 mm, and 30 mm are examined. Table 4.1 provides a summary of the simulations conducted for the solid and air within the ECU mesh sizes.
Since the aim of the study is to do a qualitative analysis with a generic model, the base size of 3 mm is chosen to save computational time. It is observed that the flow around the ECU is rather unaffected by the size of the bulk mesh of the air outside the ECU.

Base Size(mm)	Cell Count($\times 10^6$)	$T_{max}(^\circ C)$	$T_{case}(^\circ C)$
1	7.77	91.3	53.0
3	1.22	91.8	53.0
5	0.75	96.9	53.0

Table 4.1: Mesh study summary of ECU

4.1.2 Parametric Study

For the generic ECU model, the maximum allowable working temperature is defined as 120°C. The temperature of the air around the ECU is assumed to not drop below 10°C. Therefore, simulations are not conducted below this lower temperature limit. The parameters studied in the preliminary investigation are ambient temperature and fan speed.
When the fan is switched on, the maximum temperature of the ECU exhibits a linear increase with the ambient temperature, as illustrated in Fig. 4.1(a). Fig. 4.1(b) shows how the heat rejected by ECU varies with the ambient temperature. It can be observed that heat rejected by the ECU increases with the increase in the ambient temperature, which is expected due to the heat function modeled for the SoC. With the increase in the fan speed, the maximum temperature of the ECU drops as expected due to the increased convective heat transfer. It is observed

that the maximum ambient temperature limit for the functioning of the ECU is approximately 40°C.

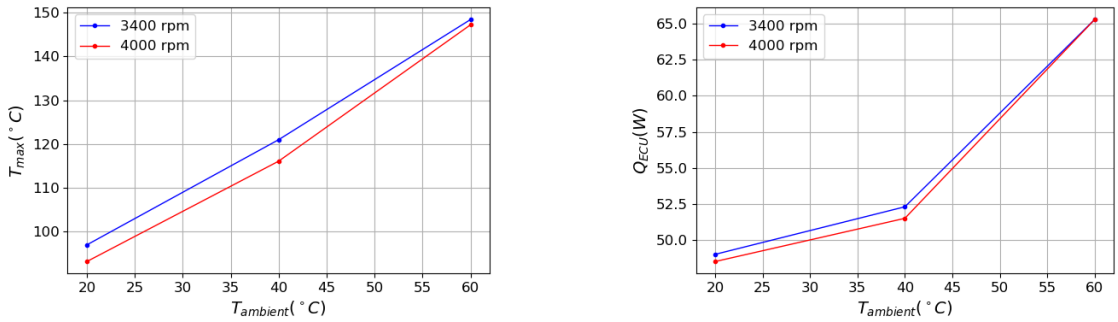

(a) (b)

Figure 4.1: Variation of temperature, and heat rejected by ECU for two fan speeds

In the case of natural convection, it is observed that the maximum temperature of the ECU reaches 180°C when the ambient temperature is set to 10°C. Therefore, heat rejection via natural convection for the set heat source values for the steady-state condition can result in the failure of the device. Hence, the fan is an essential component for the functioning of the ECU.
It is observed that the parts that are connected to the ECU case are at much lower temperatures than the components that are exposed to the air as shown in Fig. 4.2. The case of the ECU acts as a heat sink and helps in effectively rejecting heat to the ambient.

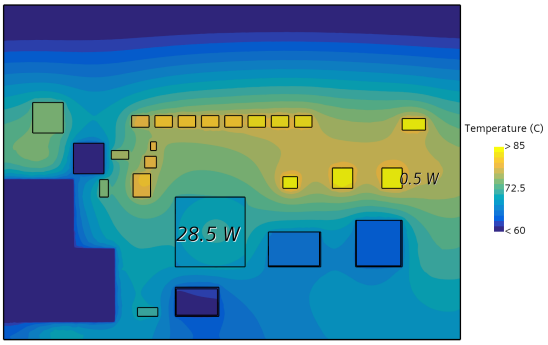

Figure 4.2: Temperature of PCB at $T_{ambient}$=20°C

4.2 Cabin Modeling

4.2.1 Mesh Study

For the mesh sensitivity analysis of the cabin, the simulation is modeled with a case setup for an ambient temperature of 0°C with a recirculation fraction of 0.1 and

HVAC temperature of 25°C. To simplify the meshing procedure both the cabin and the HVAC system are meshed with the same base size. Base sizes of 5 mm, 8 mm, and 15 mm are considered for the cabin and HVAC. To assess mesh independence, temperature along line probes at 4 locations, namely recirculation inlet, IP, floor, and ECU are monitored. It is observed that the temperature variation did not change significantly along the probes for all three cases. However, the temperature of the probe PL and the reference temperature used for the controller showed oscillations for the base size of 15 mm, Fig. 4.3. Hence, the base size of 8 mm is used for further studies, which has a cell count of approximately 14 million, Fig. 4.4.

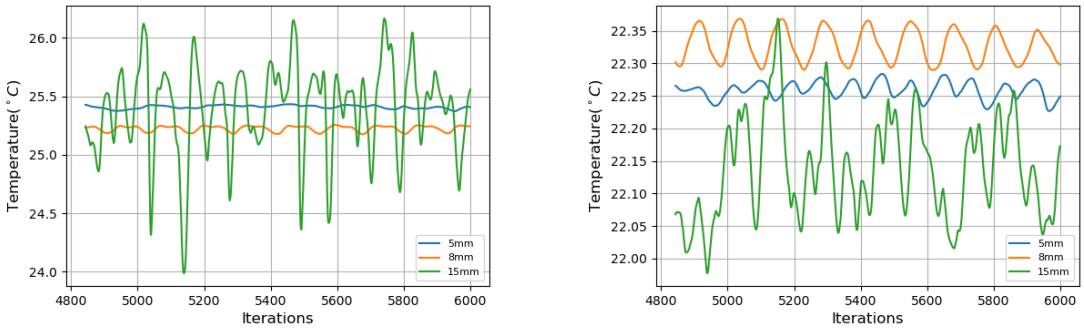

Figure 4.3: Temperature vs Iterations for different base sizes. (a)PL. (b)Reference sphere.

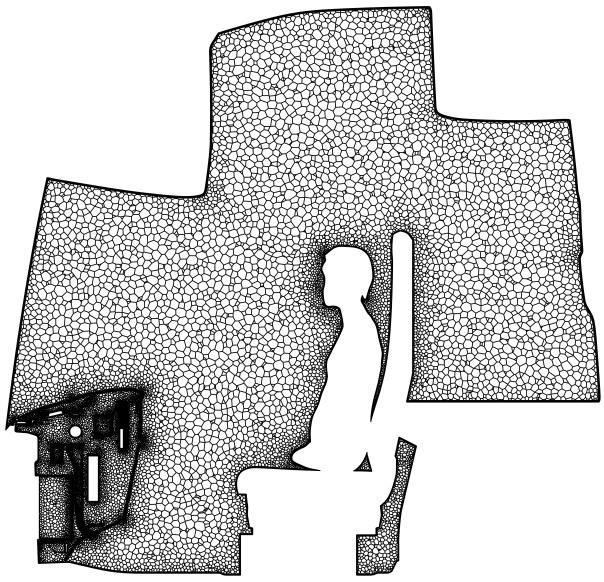

Figure 4.4: Y-plane view of cabin mesh

4.2.2 Validation of CFD model, and Controller

The validation model is simulated for ambient temperature cases of 0°C, and 35°C. The controller is initialized with HVAC temperature of 22°C for both cases. Fig. 4.5 shows how the controller adjusts the HVAC temperature to reach the set temperature of 22°C for both cases. It could be seen that the temperature of the HVAC and the reference temperature reach a converged value and have minimal fluctuations. Fig. 4.6 illustrates the temperature profile inside the cabin, and it is clear that the cabin temperature has reached the set value of 22°C, which validates the location of the sphere to represent the overall cabin temperature. Hence, the controller is considered validated.

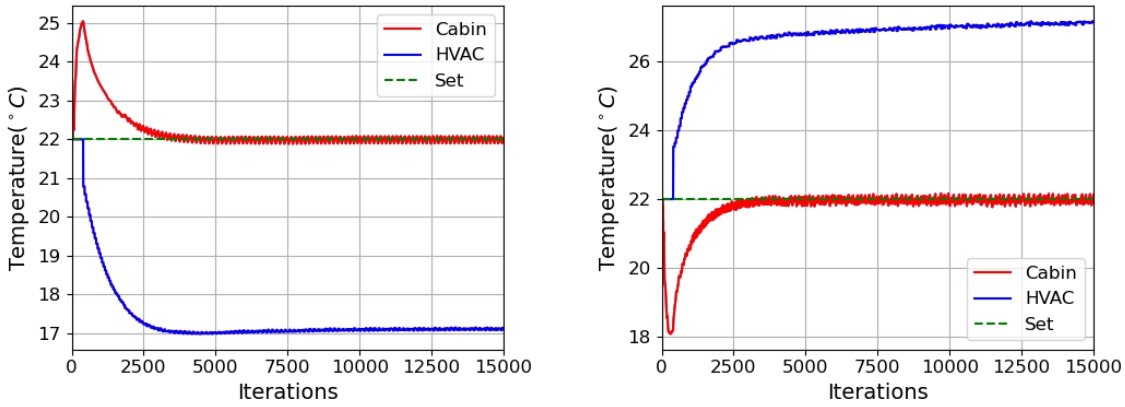

(a) (b)

Figure 4.5: Controller Performance. (a)Hot Climate. (b)Cold Climate.

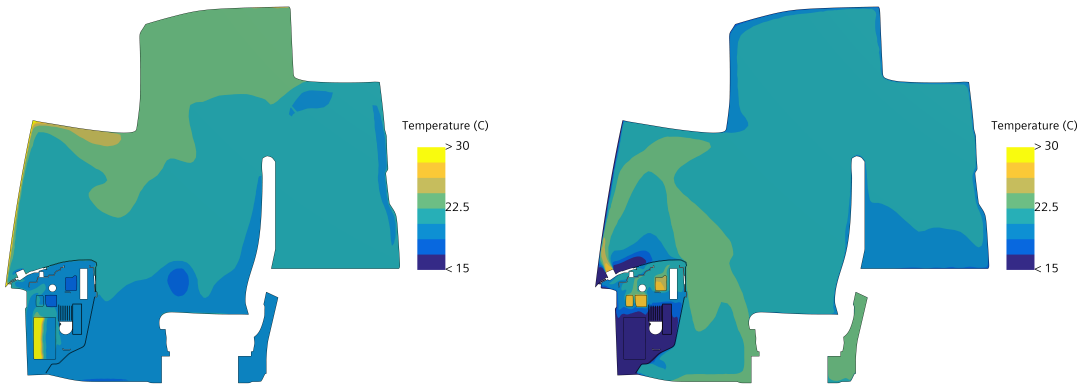

(a) (b)

Figure 4.6: Y-plane view of cabin. (a)Hot Climate. (b)Cold Climate.

Fig. 4.7 illustrates how well the simulation fits the measured data for both cases. The temperature of the air at most of the monitored points showed a good correlation with measurements.

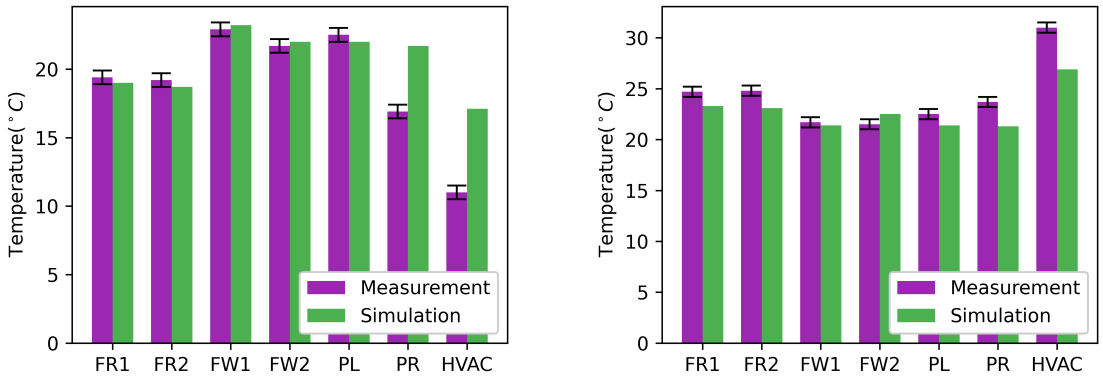

(a) (b)

Figure 4.7: Comparison of simulation and measurement. (a)Hot Climate. (b)Cold Climate.

It can be seen that for the hot climate scenario, there is an over-prediction of the temperature at probe PR. A possible reason for this deviation is that the orientation of the flaps on the right face vent for the simulation is different from its orientation when the measurement was made, affecting the accuracy of the result. In addition, there is an observed deviation in the HVAC inlet temperature in the simulation model from the measurements for both scenarios. This can be accounted to the following factors,

- Leakages - The simulations do not account for ambient air leaking into the cabin nor the cabin air leaking out of the cabin.
- One-Dimensional Thermal Conduction - The approximation of planar geometry does not fit all cabin walls. For example, cross beams in the rear wall which could result in a thermal short circuit are not accounted for in the modeling.
- Natural Convection - Due to the complexity of geometry, accurate modeling of natural convection in the enclosure is difficult.
- Measurement - It is difficult to attain a steady state in a truck cabin due to the high thermal mass of the components.

The study that is being conducted is to understand the temperature distribution of ECU qualitatively. Therefore, the CFD model can be considered validated for this study.

4.3 Cabin Study

A parametric study of the truck cabin is undergone to understand for which ambient conditions the performance of the ECU will be severely affected. The parametric study can be broadly classified as,

- Cold Climate
- Hot Climate

For each of the scenarios mentioned above, the vehicle speed, recirculation fraction, and ambient temperatures are varied to understand the effect of it on the maximum temperature of the ECU.

4.3.1 Cold Climate

4.3.1.1 Baseline

In the cold climate scenario, a truck at a standstill in an ambient temperature of 0°C is taken as the baseline simulation. The recirculation fraction is set to 0, as recirculation can result in the fogging of windows and windshields in cold climates. The key results from the simulation that are of interest for this study are:

- Temperature of HVAC air
- Maximum temperature of ECU

The low thermal conductivity of the IP, the hot air flowing through the HVAC ducts, and the confined space created by the geometry contribute to the formation of a hot pocket of air underneath the panel, as depicted in Fig. 4.8. Consequently, the air surrounding the ECU becomes hotter than the cabin temperature in this scenario, leading to higher temperatures for the ECU components. In the baseline case, the maximum temperature of the ECU is observed to be 112.0°C.

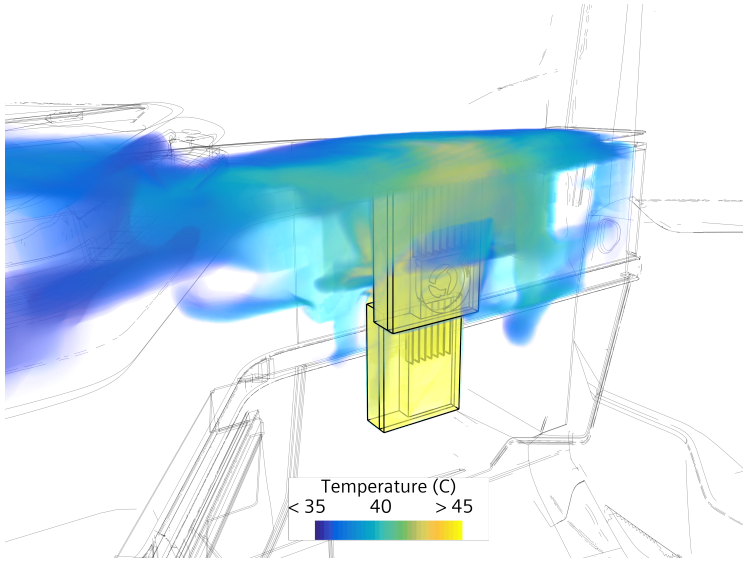

Figure 4.8: Hot air pocket underneath IP in cold ambient scenario

Additionally, due to buoyancy, thermal stratification can be observed in this scenario, as depicted in Fig. 4.9(a). Since the ECU is positioned just beneath the IP, it lies within the hotter layers. This contributes to the higher temperature of the ECU components.

4.3.1.2 Recirculaton

The baseline scenario mentioned above is simulated with a recirculation fraction of 0.5. Fig. 4.10 shows the comparison between the two cases, and it can be observed that there is a decrease in the maximum temperature of ECU with recirculation. This decrease can be attributed to enhanced air mixing from recirculation, which disrupts the thermally stratified layers, as shown in Fig. 4.9(b). The recirculation blower also functions as an exhaust mechanism to remove the hot air trapped in the instrumentation panel, as shown in Fig. 4.11(a). In this case, the recirculation removes the hot air around the 50 W ECU, which the fan of the ECU would have otherwise taken in. Additionally, recirculation increases the velocity of air around the ECU, enhancing convective heat transfer.

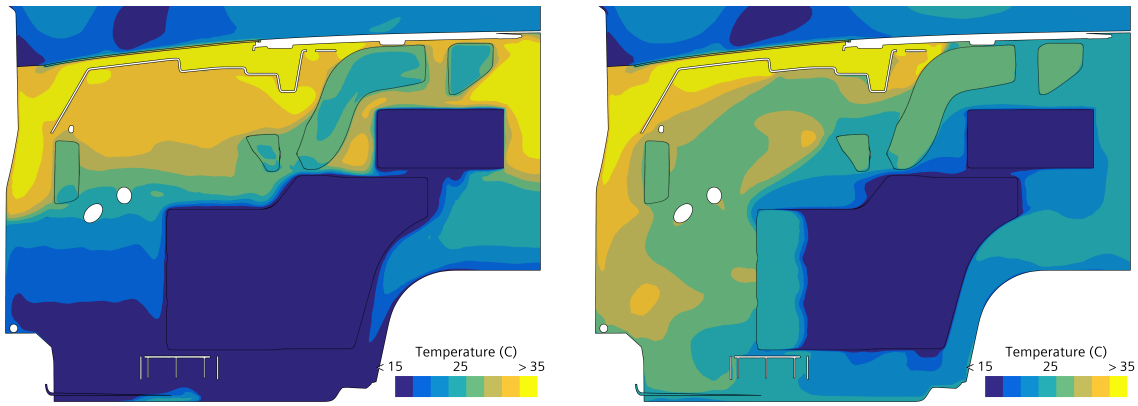

(a) (b)

Figure 4.9: X-plane view of IP. (a)Thermal stratification. (b)Mixing of layers.

A subsequent simulation with a higher recirculation fraction of 0.8 is analyzed. The temperature of the air entering the recirculation ducts increased from 24.6°C to 25.5°C with the higher recirculation fraction, Fig. 4.11(b). This indicates that increased recirculation facilitates the ventilation of more hot air through the recirculation duct, thereby reducing the temperature of the air inside the instrumentation panel. This leads to a further reduction in the temperature of the ECU components, Fig. 4.10. It should be noted that in the actual HVAC system, the recirculation duct includes the recirculation flap, and a blower, which in the simulation is modeled using a mass flow inlet. Therefore, the flow through the duct is representative of the simplified model.

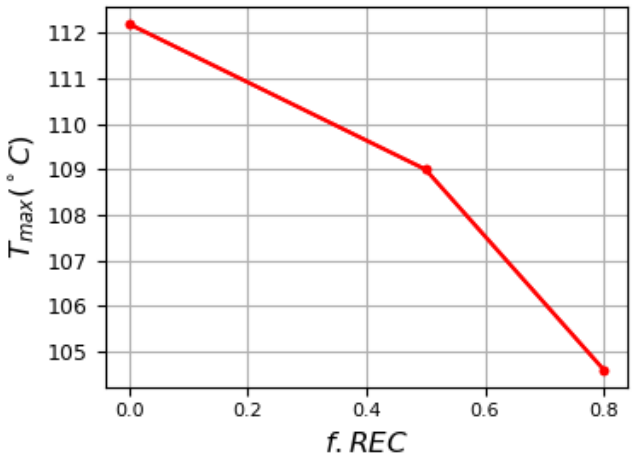

Figure 4.10: Cold climate: Maximum temperature of ECU vs. $f.REC$

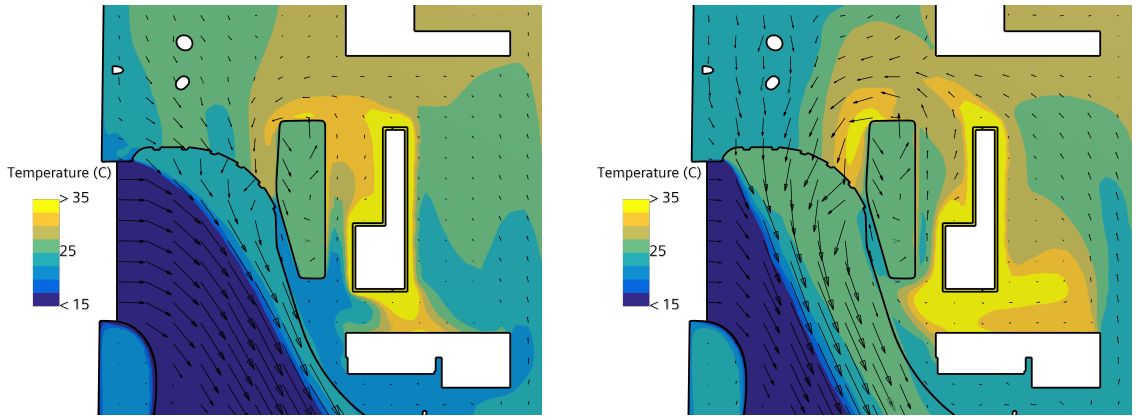

(a) (b)

Figure 4.11: Z-plane view of recirculation duct. (a)$f.REC = 0.5$. (b)$f.REC = 0.8$.

4.3.1.3 Vehicle Speed

Following this, a simulation is conducted for a truck traveling at 25 m/s with the rest of the parameters as that of the baseline. With increased vehicle speed, the convective heat transfer to the ambient through the exterior surfaces rises by around 21%. To compensate for the increased heat loss and maintain the set cabin temperature, the temperature of the air through the HVAC ducts is increased. However, due to the relatively small increase in convective loss magnitude, the resulting rise in air temperature within the HVAC ducts is not substantial (Fig. 4.12). As a result, there is minimal fluctuation in the temperature of the air inside the IP, resulting in negligible variations in the temperature of the ECU components.

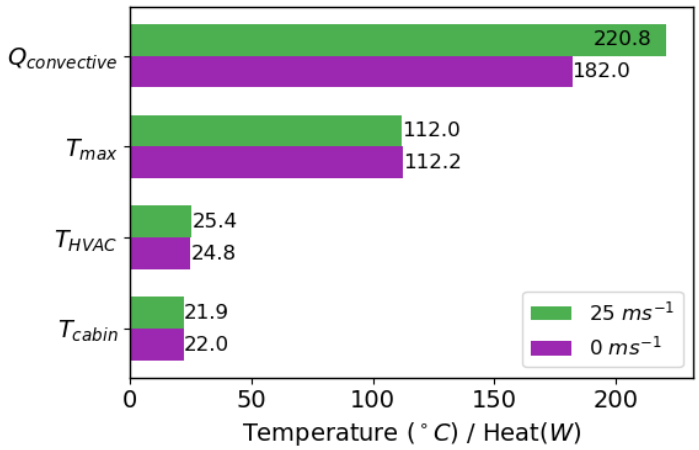

Figure 4.12: Cold climate: Summary of vehicle speed cases

4.3.1.4 Ambient Temperature

Finally, for the cold climate scenario, a lower ambient temperature of -30°C is simulated. Due to the colder ambient temperature, convective heat transfer through the cabin exterior increases significantly, approximately 1.5 times higher than the baseline. Hence, hotter air needs to be passed through the ducts to maintain the cabin at 22°C, Fig. 4.14. However, contrary to previous results, the temperature of the ECU components shows a decrease. In a cold climate, the cold ambient air will pass through the recirculation duct, which cools its surrounding air. Due to the proximity of the ECU to the recirculation duct(illustrated in Fig. 3.9), its centrifugal fan draws in this cold air as shown in Fig. 4.13. As the ambient temperature drops, the temperature of the air through the recirculation duct decreases further, resulting in an even cooler intake by the fan. This leads to the observed decrease in the temperature of the ECU components.

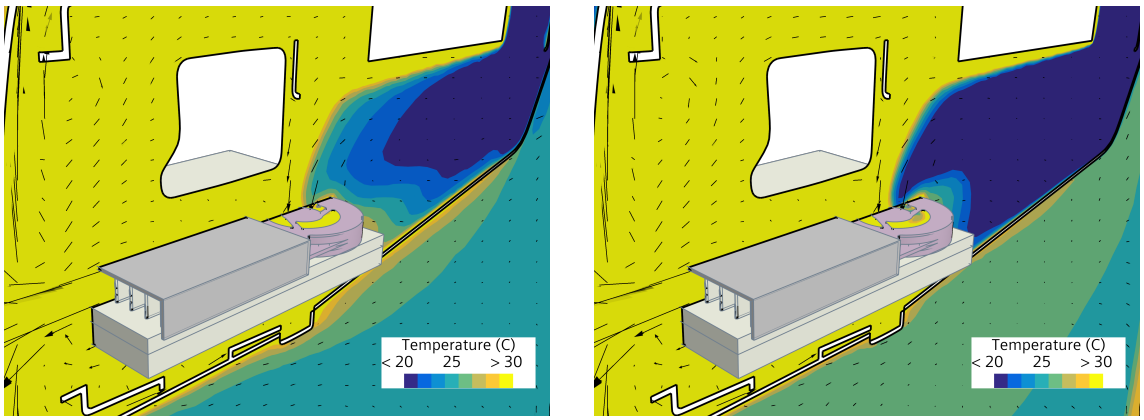

(a) (b)

Figure 4.13: Y-plane view of air around ECU. (a)$T_{ambient} = 0°C$. (b)$T_{ambient} = -30°C$.

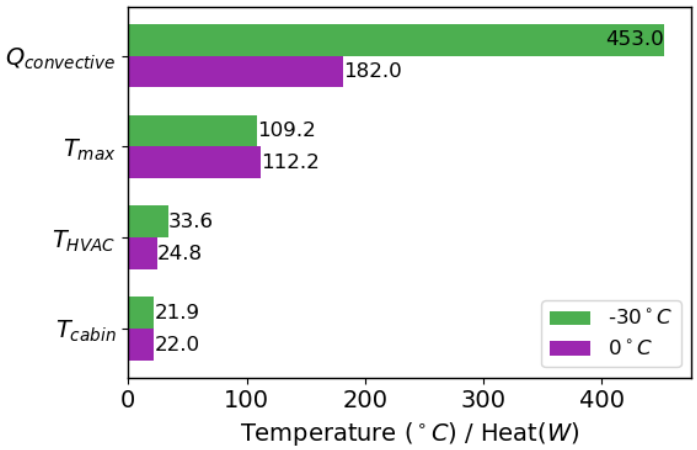

Figure 4.14: Cold Climate: Summary of ambient temperature cases

4.3.2 Hot Climate

4.3.2.1 Baseline

A typical hot climate scenario, where a truck is at a standstill, is used as the baseline for the hot climate simulation. The simulation is set with an ambient temperature of 35°C. Since recirculation can be utilized in hot climates to conserve energy without the risk of fogging, the recirculation fraction is set to 0.83. Similar to the previous climate study, the maximum temperature of the ECU and the HVAC outlet temperature are analyzed.
A hot air pocket forms underneath the IP due to the heat rejected by the ECUs, as shown in Fig. 4.15.

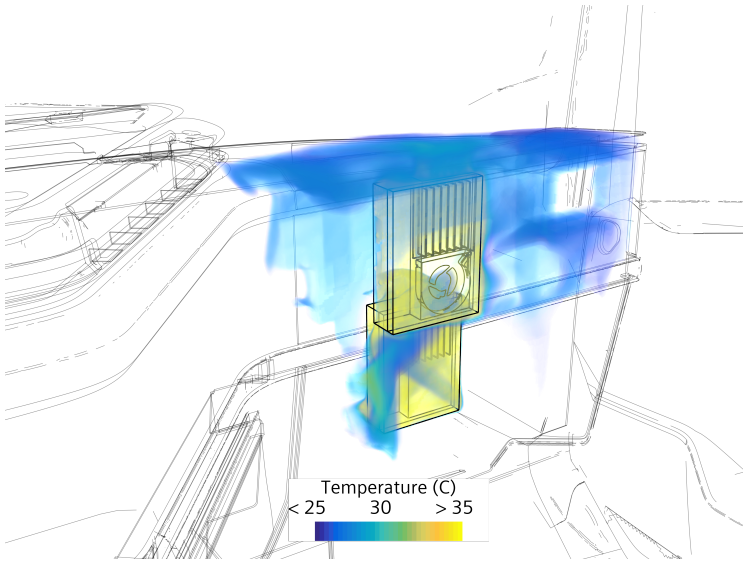

Figure 4.15: Hot air pocket underneath IP in hot ambient scenario

Compared to the cold case, the temperature of the air underneath the IP is significantly lower. This is due to the high recirculation fraction at which the HVAC

operates in a typical hot climate scenario, and the cold air through the HVAC ducts acting as a heat sink that takes in the heat generated by the ECU. The maximum temperature of the ECU for this scenario is 95.2°C, and the HVAC temperature is 13.9°C.

4.3.2.2 Recirculation

A study is conducted to analyze how the recirculation fraction affects the temperature of the air next to the ECU. For this, cases with a recirculation fraction of 0.5 and 0 are simulated. As expected, decreasing the recirculation fraction leads to less air inside the IP venting out through the recirculation duct, which leads to an increase in the temperature of the air inside the IP. This results in a rise in the temperature of the ECU components. Fig. 4.16 illustrates the variation in the maximum temperature of ECU components with recirculation fraction.

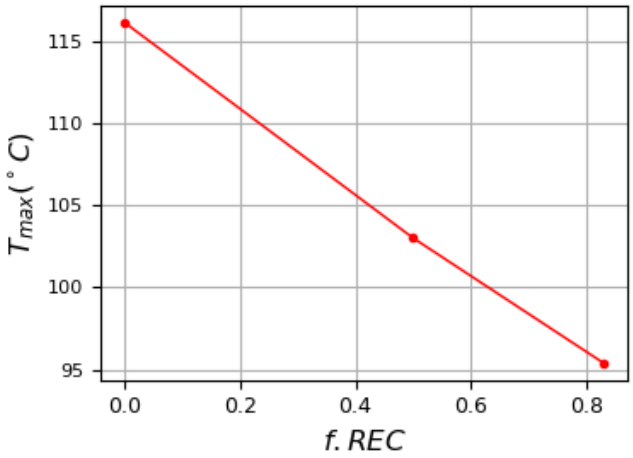

Figure 4.16: Hot climate: Maximum temperature of ECU vs. $f.REC$

4.3.2.3 Vehicle Speed

A simulation is performed to understand the effect of vehicle speed on the ECU temperature at 25 m/s. At higher speeds, the convective heat transfer coefficient of the cabin exterior rises, requiring additional cooling power to keep the cabin temperature at 22°C. This results in a decrease in the temperature of the air flowing through the ducts, as shown in Fig. 4.17. Similar to the scenario in cold climates, the variation in HVAC temperature with different vehicle speeds is minor. Hence, the ECU temperature does not experience significant changes in this situation.

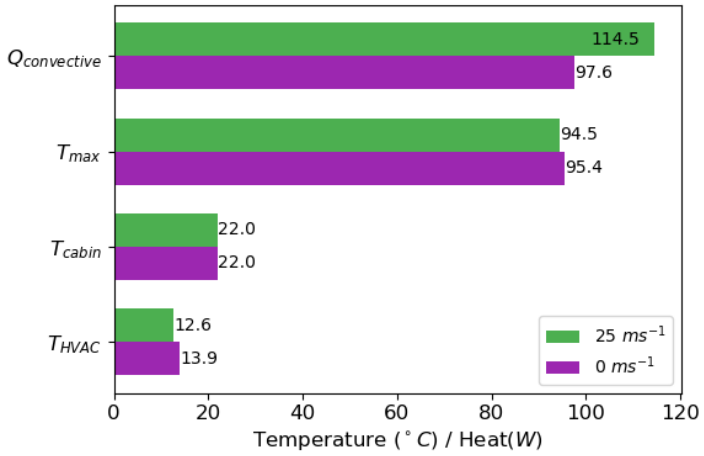

Figure 4.17: Hot climate: Summary of vehicle speed cases

4.3.2.4 Ambient Temperature

Finally, a simulation is conducted for a truck at an ambient temperature of 45°C to understand the influence of an increase in ambient temperature. At a higher ambient temperature, more heat will be transferred into the cabin. Hence, the temperature of the air through ducts will need to be reduced to maintain the cabin at the set temperature, as shown in Fig. 4.18. The temperature of the air around the ECU decreases because of its proximity to the ducts, which results in a decrease in the maximum temperature of the ECU.

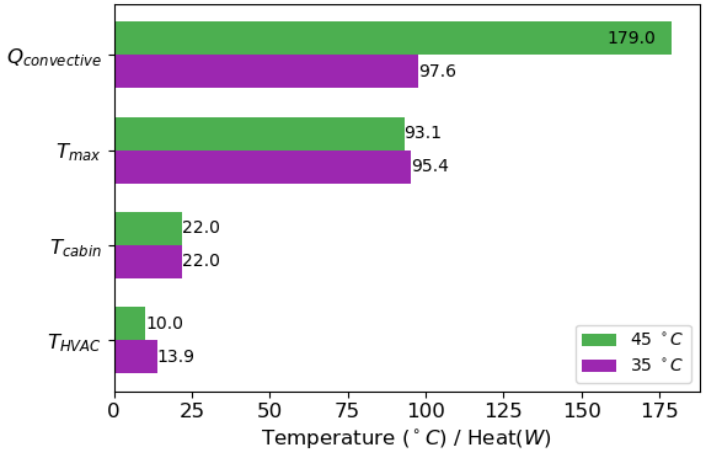

Figure 4.18: Hot climate: Summary of ambient temperature cases

4.3.3 Summary

A summary of the cabin study is explained in this section. Figure 4.19 illustrates how the maximum temperature of the ECU varies with recirculation fraction and ambient temperature. It is clear that regardless of the ambient temperature, an increase in the recirculation fraction results in a decrease in the temperature of the ECU components.

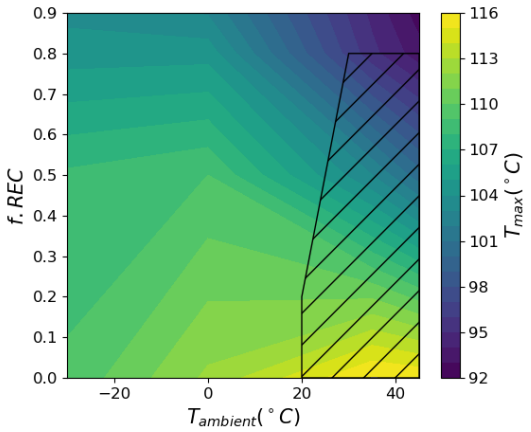

Figure 4.19: Variation of T_{max} with $T_{ambient}$ and $f.REC$

Based on the study, the worst-case scenario for the ECU occurs when the ambient temperature is high and there is no recirculation. However, to conserve energy, trucks are typically operated with high recirculation fractions in hot climates. Therefore, in practice, the hatched region will not be utilized, ensuring that the ECU operates safely under hot climate conditions.

Conversely, a typical cold climate scenario would involve no recirculation at all as a preventive measure against fogging. Due to the same, in reality, cold climates would result in higher temperatures for the ECU components. The slight decrease in temperature with a drop in ambient temperature is due to specific phenomena mentioned in section 4.3.1.4. If the ECUs were located in a more isolated position within the IP, the trend of increasing ECU temperature with decreasing ambient temperature would have been more pronounced.

It can also be observed that the rate of change in ECU temperature with $f.REC$ decreases as the ambient temperature drops. This means that the impact of increased recirculation on reducing ECU temperature is minimal in cold ambient conditions. Therefore, if the component temperatures are at the limit of their operating range, relying solely on recirculation is not a viable cooling solution. Finally, it is observed that the gain or loss of thermal energy of the cabin with a change in vehicle velocity is not significant, and the temperature of the air in ducts does not vary a lot compared to the case of changing ambient temperature.

4.4 Cooling Strategies

Based on the parametric study of the cabin, several conclusions can be drawn regarding the reasons for the increase in the temperature of ECU components. By understanding these phenomena, strategies can be devised to reduce the temperature of the ECU. The strategies are classified into two:

- Passive - Improving cooling performance using existing geometry
- Active - Use of external cooling solutions

4.4.1 Passive Method

4.4.1.1 Location of ECU

Positioning the ECU in locations where the air around it is cold, and regions with relatively higher fluid flow can help in keeping the ECU cool. For example, locations closer to the cabin floor will have colder air compared to the regions just underneath the IP. If there is a possibility for recirculation, positioning the ECU close to that region could be beneficial due to the higher fluid flow in that region.

4.4.1.2 Orientation of ECU

As discussed in section 4.3.1.2, the mixing of air results in a decrease in the temperature of the air around the ECU. One way to achieve this mixing is by inverting the ECU. The centrifugal fan of the ECU draws in the hot air in the upper layer and mixes it with cold air in the bottom, as illustrated in Fig. 4.20(b). This mixing is shown to reduce the maximum temperature of the ECU by 5.1°C.
However, the effectiveness of this method depends on the position of the ECU within the thermal layers. If the ECU is located in cooler layers, mixing might increase the air temperature around the ECU, leading to higher temperatures, contrary to the above-obtained results.

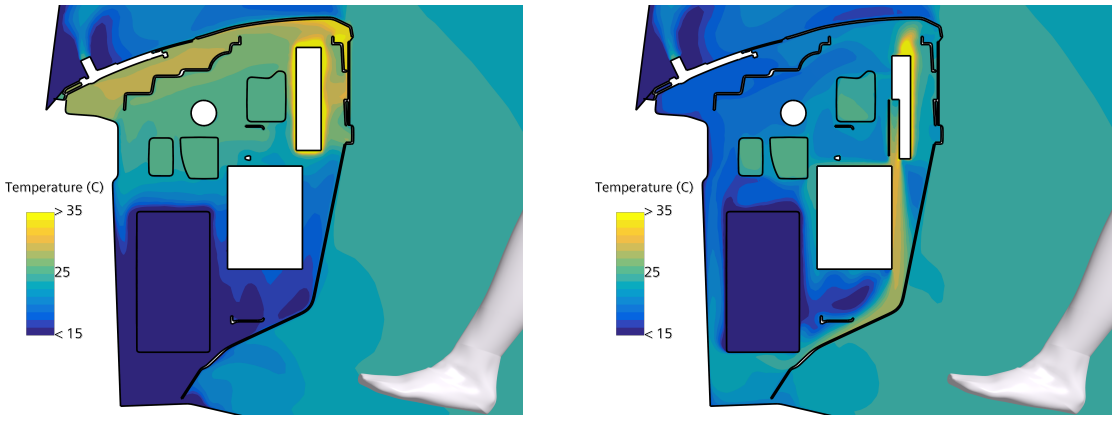

(a) (b)

Figure 4.20: Y-plane view of IP. (a)Baseline. (b)Inverted ECU.

4.4.2 Active Method

4.4.2.1 Cooling Ducts

One highly effective method to cool down the ECU is by directing cold air onto it. The parametric study revealed that the worst-case scenario for the ECU occurs when the ambient temperature is low. Therefore, by adding a duct to the HVAC system, cold ambient air can be directed specifically onto the ECU. However, this solution adds more requirements and design changes to the HVAC system which need to be considered.

4.4.2.2 External Fan

Using an external fan to induce mixing inside the IP instead of using the ECU is also a viable option to cool the ECU. An axial fan(fan curve in Fig. 4.22) is placed underneath the IP (highlighted in Fig. 4.21(b)), away from the ECU. This fan draws in hot air from the top and directs it to the cabin floor. This mixing effectively reduces the air temperature around the ECU, lowering its maximum temperature by 8°C.

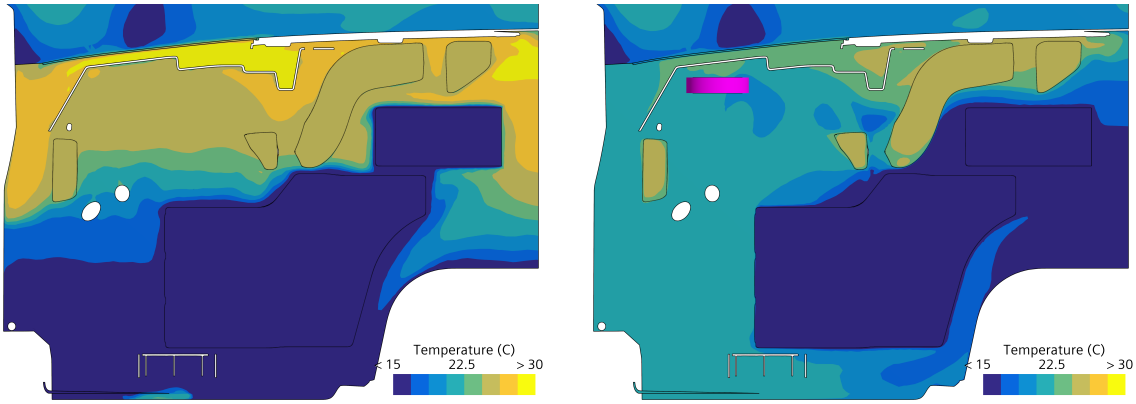

(a) (b)

Figure 4.21: X-plane view of IP. (a)Baseline. (b)With Axial Fan.

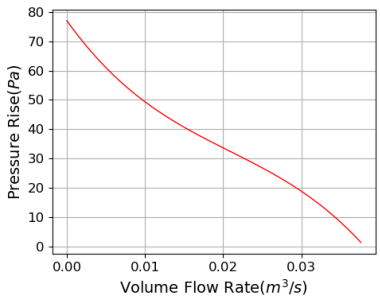

Figure 4.22: Fan curve at the rotation speed of 3000 rpm

5
Conclusion

In this study, the thermal behavior of a generic ECU was analyzed using steady-state CFD simulations. For the generic ECU to function within its set operating range, the fan of the ECU is essential, and the temperature of the air around the ECU should be below approximately 40°C.

The PI controller that was modeled to regulate the air temperature through the HVAC ducts to maintain the cabin temperature at 22°C is robust. Due to the low thermal conductivity of the IP, the heat generated by the heat sources inside it forms a hot air pocket that impacts the ECU's temperature. The air flowing through the HVAC ducts, which serve as the primary heat source and sink, influences the ECU's temperature due to its proximity.

It can be concluded that the coupled effect of hot air through the HVAC ducts combined with no recirculation in cold ambient conditions results in high temperatures for ECU components. Thermal stratification was observed, indicating the temperature of the ECUs positioned in the hotter layers, can be reduced through air mixing. Recirculation, which enhances air mixing inside the IP, and vents out the hot air decreased the ECU's temperature. At an ambient temperature of 0°C, increasing the recirculation fraction from 0 to 0.8 reduced the ECU's maximum temperature by approximately 7°C.

Due to the limitations of using recirculation in cold ambient conditions, some cooling strategies were proposed to improve the thermal management of ECUs. Enhancing air mixing within the IP using the existing fan of the ECU reduced the ECU's temperature by around 5°C. Incorporating an additional fan provided an even greater reduction, lowering the temperature by approximately 8°C. Since the ECU's temperature is influenced by local phenomena, developing a universal cooling strategy is challenging. However, the findings from this study offer insights into considerations for effective thermal management of ECUs inside a truck cabin.

As part of the project's future scope, it is essential to investigate the transient thermal behavior of the ECU within the cabin. Two critical worst-case scenarios are not addressed in this study: the transient thermal response of the ECU after the cabin has been soaked in cold and hot climates. The radiation to the environment and the modeling of solar loads are factors worth considering.

Bibliography

[1] V. Lakshminarayanan and N. Sriraam. "The effect of temperature on the reliability of electronic components". In: *2014 IEEE International Conference on Electronics, Computing and Communication Technologies (CONECCT)*. 2014, pp. 1–6. DOI: 10.1109/CONECCT.2014.6740182.

[2] H Versteeg and W Malalasekera. *An introduction to computational fluid dynamics*. en. 2nd ed. Philadelphia, PA: Prentice Hall, Feb. 2007.

[3] *Siemens Digital Industries Software. (2020). Simcenter STAR-CCM+ Documentation Version 2020.3.*

[4] V. Lemort, G. Olivier, and G. de Pelsemaeker. *Thermal Energy Management in Vehicles*. Automotive Series. Wiley, 2023. ISBN: 9781119251743. URL: https://books.google.se/books?id=Md2lEAAAQBAJ.

[5] *NPTEL.Mechanical engineering - Refrigeration and Air Conditioning*. URL: https://archive.nptel.ac.in/courses/112/105/112105129/#.

[6] K.J. Åström and R. Murray. *Feedback Systems: An Introduction for Scientists and Engineers, Second Edition*. Princeton University Press, 2021. ISBN: 9780691213477. URL: https://books.google.se/books?id=qZ0DEAAAQBAJ.

[7] Anandh Ramesh Babu et al. "An adaptive cabin air recirculation strategy for an electric truck using a coupled CFD-thermoregulation approach". In: *International Journal of Heat and Mass Transfer* 221 (2024), p. 125056.

[8] Simcenter STAR-CCM+. "KB Article ID KB000130384_EN_US".

[9] Volupe. "Wall Y+ Calculator.".

[10] Yunus A Cengel and Afshin J Ghajar. *Heat and mass transfer: Fundamentals and applications*. 5th ed. New York, NY: McGraw-Hill Professional, Apr. 2014.

[11] Paul Danca et al. "On the Possibility of CFD Modeling of the Indoor Environment in a Vehicle". In: *Energy Procedia* 112 (2017), pp. 656–663.

[12] Siemens Support Knowledge Base: Implementing a Proportional-Integral (PI) controller in STAR-CCM+.

A

Auxiliary Visuals

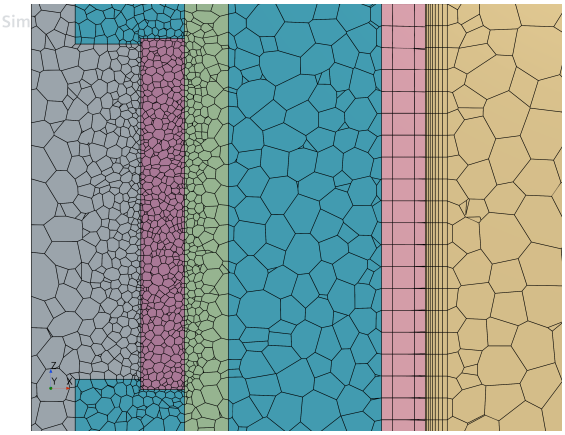

Figure A.1: Section view of ECU and air mesh

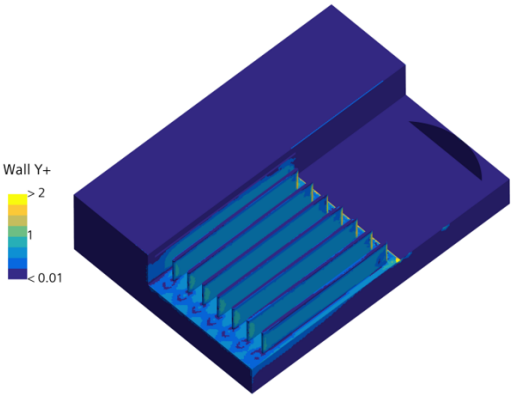

Figure A.2: Wall y^+ of ECU at $\omega = 4000$ rpm(Preliminary Study)

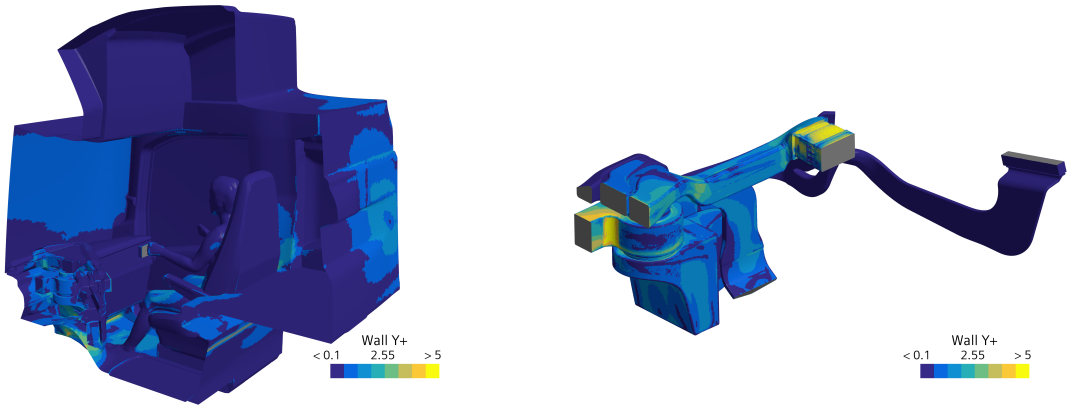

(a) (b)

Figure A.3: Wall y^+ of validation model(hot climate). (a)Cabin Interior. (b)HVAC.

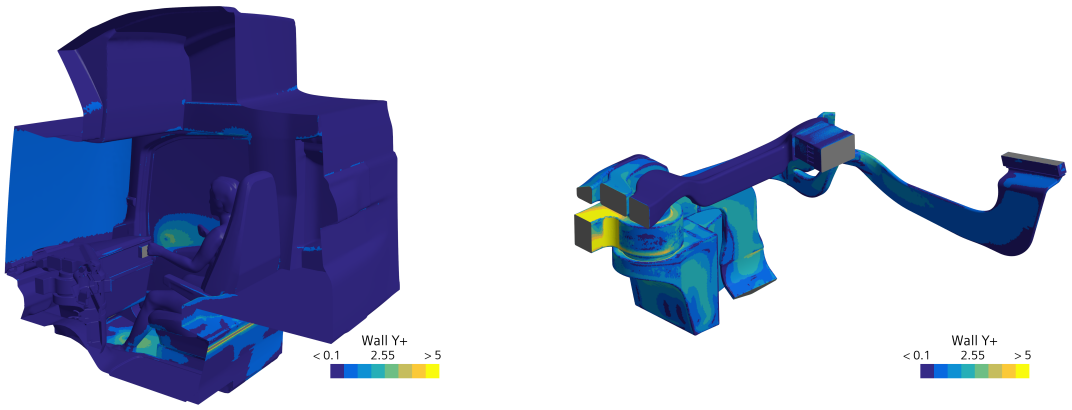

(a) (b)

Figure A.4: Wall y^+ of validation model(cold climate). (a)Cabin Interior. (b)HVAC.

B

Boundary Conditions

Boundary Condition	Surface
Wall(constant temperature)	Enclosure walls

Table B.1: Boundary conditions used for preliminary study

Boundary Condition	Surface
Wall(convection)	Cabin walls
Wall(constant temperature)	Manikin
Wall(adiabatic)	Curtain, Harness, Seat
Mass flow inlet	HVAC vents, Recirculation inlet(HVAC side)
Pressure outlet	Evacuation, Recirculation outlet
Outlet(specified mass flow)	Recirculation inlet(cabin side)
Symmetry plane	Half plane

Table B.2: Boundary conditions used for cabin study

DEPARTMENT OF MECHANICS AND MARITIME SCIENCES
CHALMERS UNIVERSITY OF TECHNOLOGY
Gothenburg, Sweden 2024
www.chalmers.se

CHALMERS
UNIVERSITY OF TECHNOLOGY